Cranial anatomy of Yinlong downsi (Ornithischia: Ceratopsia) from the Upper Jurassic Shishugou Formation of Xinjiang, China

Article *in* Journal of Verterbrate Paleontology · November 2015

DOI: 10.1080/02724634.2015.1029579

4 authors, including:

Catherine A Forster
George Washington University

James M Clark
George Washington University

Xing Xu
Chinese Academy of Sciences

Journal of Vertebrate Paleontology

ISSN: 0272-4634 (Print) 1937-2809 (Online) Journal homepage: http://www.tandfonline.com/loi/ujvp20

Cranial anatomy of Yinlong downsi (Ornithischia: Ceratopsia) from the Upper Jurassic Shishugou Formation of Xinjiang, China

Feng-Lu Han, Catherine A. Forster, James M. Clark & Xing Xu

To cite this article: Feng-Lu Han, Catherine A. Forster, James M. Clark & Xing Xu (2015): Cranial anatomy of Yinlong downsi (Ornithischia: Ceratopsia) from the Upper Jurassic Shishugou Formation of Xinjiang, China, Journal of Vertebrate Paleontology, DOI: 10.1080/02724634.2015.1029579

To link to this article: http://dx.doi.org/10.1080/02724634.2015.1029579

Journal of Vertebrate Paleontology e1029579 (27 pages)

DOI: 10.1080/02724634.2015.1029579

ARTICLE

CRANIAL ANATOMY OF *YINLONG DOWNSI* (ORNITHISCHIA: CERATOPSIA) FROM THE UPPER JURASSIC SHISHUGOU FORMATION OF XINJIANG, CHINA

FENG-LU HAN,[1,2,*] CATHERINE A. FORSTER,[3] JAMES M. CLARK,[3] and XING XU[2]
[1]School of Earth Sciences, China University of Geosciences, 388 Lumo Road, Wuhan 430074, People's Republic of China, hfl0501@gmail.com;
[2]Key Laboratory of Vertebrate Evolution and Human Origins of Chinese Academy of Sciences, Institute of Vertebrate Paleontology and Paleoanthropology, Chinese Academy of Sciences, 142 Xizhimenwai Street, Beijing 100044, People's Republic of China, xingxu@vip.sina.com;
[3]Department of Biological Sciences, The George Washington University, 2023 G Street Northwest, Washington, DC 20052, U.S.A, forster@gwu.edu; jclark@gwu.edu

ABSTRACT—*Yinlong downsi*, from the Upper Jurassic Shishugou Formation, Xinjiang, northwestern China, is the oldest known ceratopsian dinosaur. Here we provide a detailed description of the skull and mandible based on the holotype, three partial skulls, and disarticulated materials from several other specimens. *Yinlong* can be diagnosed by six autapomorphies: a distinct fossa along the midline of the frontals; a slit-like carotid canal bordered by laminae; premaxillary teeth with a vertical wear facet and a basal shelf; a deep sulcus on the ventral surface of the quadratojugal; large oval nodules concentrated on the lateral surface of the jugal; and a squamosal with an expanded dorsal surface and a long, constricted quadrate process. A detailed comparison with other basal ceratopsians suggests that *Yinlong downsi* may belong within Chaoyangsauridae. *Yinlong* also shares many derived characters both with *Psittacosaurus* and neoceratopsians, suggesting that character evolution in early ceratopsians is complex. Additionally, a caniniform premaxillary tooth is present in one small specimen (IVPP V18636), which may suggest sexual dimorphism or individual variation.

SUPPLEMENTAL DATA—Supplemental materials are available for this article for free at www.tandfonline.com/UJVP

Citation for this article: Han, F.-L., C. A. Forster, J. M. Clark, and X. Xu. 2015. Cranial anatomy of *Yinlong downsi* (Ornithischia: Ceratopsia) from the Upper Jurassic Shishugou Formation of Xinjiang, China. Journal of Vertebrate Paleontology. DOI: 10.1080/02724634.2015.1029579.

INTRODUCTION

Marginocephalia, including pachycephalosaurs and ceratopsians, was first established by Sereno (1986). However, only three synapomorphies have supported this hypothesis (Sereno, 2000), and the close relationship between these taxa has been questioned by some authors (Dodson et al., 1990; Sullivan, 2006). Therefore, basal ceratopsians and pachycephalosaurs are critical for determining marginocephalian monophyly and relationships. Fortunately, a series of basal ceratopsians have been discovered and reported in recent years, including *Chaoyangsaurus youngi* (see Zhao et al., 1999), *Archaeoceratops oshimai* (see Dong and Azuma, 1997; You and Dodson, 2003), *Liaoceratops yanzigouensis* (see Xu et al., 2002), *Yamaceratops dorngobiensis* (see Makovicky and Norell, 2006), *Auroraceratops rugosus* (see You et al., 2005), *Xuanhuaceratops niei* (see Zhao et al., 2006), and *Yinlong downsi* (see Xu et al., 2006).

Yinlong downsi, the earliest and most complete basal ceratopsian, was originally described based on a nearly complete skull and postcranial skeleton (IVPP V14530). *Yinlong downsi* is an important species not only for its early occurrence but also for its combination of characters that provides additional evidence for the monophyly of Marginocephalia and its possible sister group relationship to heterodontosaurids (Xu et al., 2006). Heterodontosaurids are some of the most controversial taxa of ornithischians and have been proposed to be basal ornithopods (Sereno, 1999; Norman et al., 2004), the sister taxon of Cerapoda (Maryańska and Osmólska, 1985), the sister taxon of marginocephalians (Cooper, 1985; Xu et al., 2006), or the most basal ornithischians (Butler et al., 2008; Norman et al., 2011). However, the relationship between heterodontosaurids and marginocephalians has remained weakly supported (Norman et al., 2011).

Yinlong downsi was originally recovered as the basal-most ceratopsian (Xu et al., 2006; Chinnery-Allgeier and Kirkland, 2010). However, some recent ceratopsian phylogenetic analyses assign it to the Chaoyangsauridae, a clade of basal neoceratopsians, with the Early Cretaceous *Psittacosaurus* as the basal-most ceratopsian (Han, 2009; Morschhauser, 2012). Therefore, the relationship of *Yinlong* with *Chaoyangsaurus, Psittacosaurus*, and other basal neoceratopsians such as *Liaoceratops* and *Archaeoceratops* requires additional comparison and analysis.

Here we provide a detailed description of the skull and mandible of *Yinlong downsi*. All these materials were collected from the Upper Jurassic (Oxfordian) Shishugou Formation of the Wucaiwan area, Xinjiang, northwestern China (Fig. 1). Other ornithischians collected from the Shishugou Formation include *Gongbusaurus wucaiwanensis* (Dong, 1989) and, from the Jiangjunmiao area, the stegosaur *Jiangjunosaurus junggarensis* (Jia et al., 2007).

Institutional Abbreviations—IGCAGS Institute of Geology Chinese Academy of Geosciences, Beijing, China; **IVPP**, Institute of Vertebrate Paleontology and Paleoanthropology, Beijing, China; **NHMUK**, Natural History Museum, London, U.K.;

*Corresponding author.

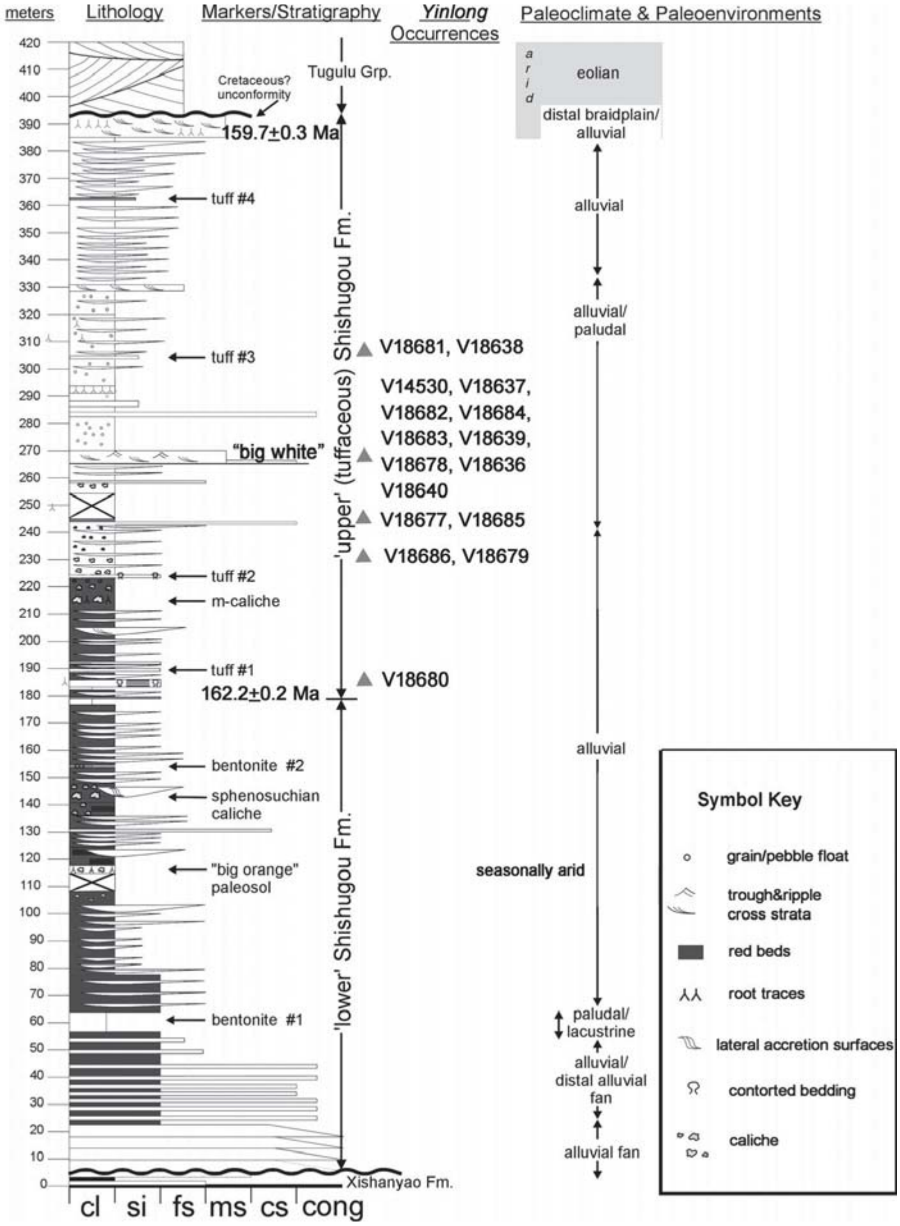

FIGURE 1. Stratigraphic section through the Shishugou Formation (modified from Eberth et al., 2010). **Abbreviations**: **cl**, claystone; **cong**, conglomerate; **cs**, coarse-grained sandstone; **fs**, fine-grained sandstone; **ms**, medium-grained sandstone; **si**, siltstone.

ZDM, Zigong Dinosaur Museum, Dashanpu, China; **ZMNH**, Zhejiang Museum of Natural History, Hangzhou, China.

SYSTEMATIC PALEONTOLOGY

ORNITHISCHIA Seeley, 1887
CERATOPSIA Marsh, 1890
CHAOYANGSAURIDAE Zhao et al., 2006
YINLONG Xu, Forster, Clark, and Mo, 2006

Type Species—*Yinlong downsi* (by monotypy).

Diagnosis—As for the type species (see below).

Locality and Horizon—Wucaiwan area, Junggar Basin, Xinjiang Uyghur Autonomous Region, northwest China. The holotype and referred specimens are from the upper part of the Shishugou Formation. The lower part of the formation was previously correlated with the late Middle Jurassic Callovian stage based on the dating of tuff T1 in the middle of the formation (Clark et al., 2006), but recalibration of the Fish Canyon sanidine (Kuiper et al., 2008) and refined dating of the Middle-Upper Jurassic boundary (Gradstein et al., 2012) now place nearly the entire formation in the Oxfordian stage of the early Late Jurassic (David Eberth, pers. comm.).

YINLONG DOWNSI Xu, Forster, Clark, and Mo, 2006
(Figs. 2–21)

Emended Diagnosis—(Cranial features only; after Xu et al., 2006.) A basal ceratopsian diagnosed by the following autapomorphies: a distinct fossa along the midline of the frontals; a slit-like carotid canal bordered by laminae; premaxillary teeth with a vertical wear facet and a basal shelf; a deep sulcus on the ventral surface of the quadratojugal; large oval nodules concentrated on the lateral surface of the jugal; and a squamosal with an expanded dorsal surface and a long, constricted quadrate process.

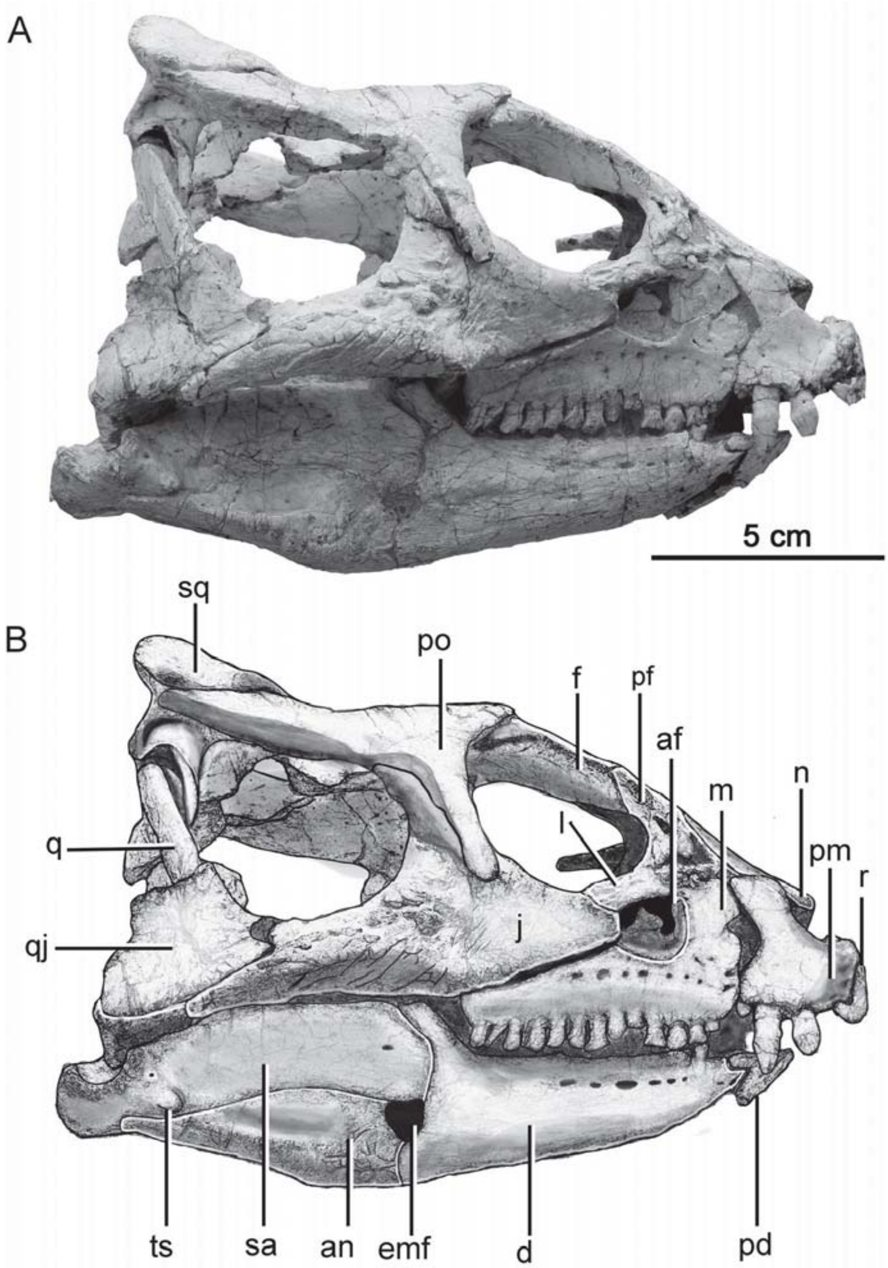

FIGURE 2. *Yinlong downsi* IVPP V14530 (holotype) skull and mandible in right lateral view. **A**, photograph; **B**, drawing. **Abbreviations**: **an**, angular; **af**, antorbital fossa; **d**, dentary; **emf**, external mandibular fenestra; **f**, frontal; **j**, jugal; **l**, lacrimal; **m**, maxilla; **n**, nasal; **pd**, predentary; **pf**, prefrontal; **pm**, premaxilla; **po**, postorbital; **q**, quadrate; **qj**, quadratojugal; **r**, rostral; **sa**, surangular; **sq**, squamosal; **ts**, tubercle on surangular.

Holotype—IVPP V14530, a nearly complete skull with mandible and nearly complete postcranial skeleton. It has a skull length (rostral to quadrate condyle) of 18 cm (Figs. 2–7, 19). The left side of the skull and mandible are gently compressed dorsoventally (Fig. 5). The occipital region is damaged; the paired exoccipitals are preserved, but most of the braincase is missing. The basioccipital and basisphenoid are co-ossified and preserved separate from the skull. The pterygoid, ectopterygoid, and palatine are partially preserved and exposed. The postcranial skeleton, exposed only in dorsal view, is missing only the distal tail and parts of the right forelimb.

Referred Materials—IVPP V18636, a nearly complete skull with mandible and partial postcranial skeleton. The skull length (rostral to quadrate condyle) is approximately 15.5 cm, or 86% of that of the holotype. The skull is gently compressed dorsoventrally, the dorsal surface is partially damaged, and much of the left side of the skull is missing or damaged (Figs. 8–10). The occiput is partially exposed, although the ventral surface of the basicranium and palate remain covered in matrix. The mandible is nearly complete but skewed laterally. The postcranial material includes articulated cervical and dorsal vertebrae and dorsal ribs and a scapula, femur, tibia, and fibula.

IVPP V18686, a complete skull and mandible, is slightly smaller than the holotype. The specimen is severely compressed dorsoventrally and exposed in dorsal and right lateral views (Fig. 11). The postcranial materials include cervical and dorsal vertebrae, pectoral girdle, and partial forelimbs.

IVPP V18638, the smallest specimen described here, consists of a partially preserved skull, a damaged femur, and a partial scapula. The skull is strongly compressed mediolaterally, and

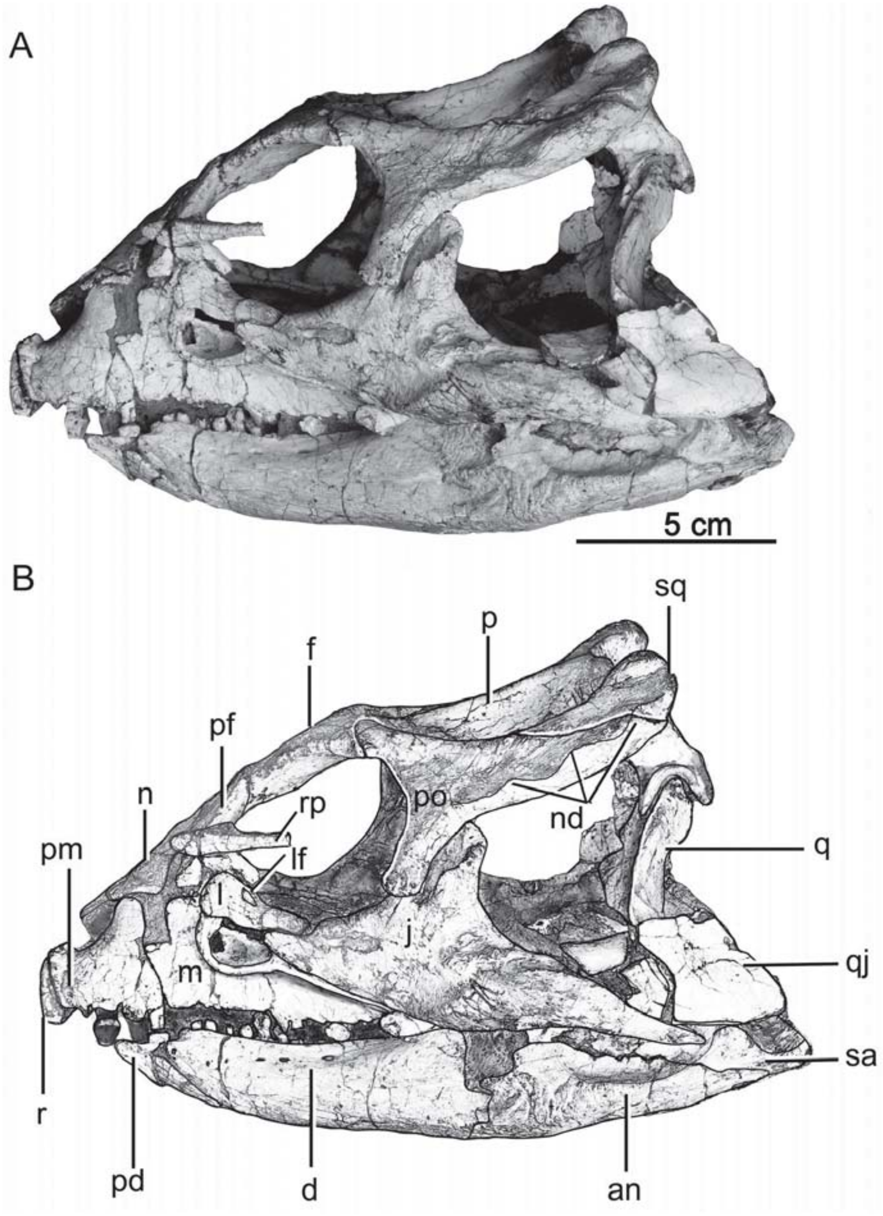

FIGURE 3. *Yinlong downsi* IVPP V14530 (holotype) skull and mandible in left lateral view. **A**, photograph; **B**, drawing. **Abbreviations**: **an**, angular; **d**, dentary; **f**, frontal; **j**, jugal; **l**, lacrimal; **lf**, lacrimal foramen; **m**, maxilla; **n**, nasal; **nd**, nodes; **p**, parietals; **pd**, predentary; **pf**, prefrontal; **pm**, premaxilla; **po**, postorbital; **q**, quadrate; **qj**, quadratojugal; **r**, rostral; **rp**, right palpebral; **sa**, surangular; **sq**, squamosal.

includes the right maxilla, jugal, squamosal, postorbital, quadratojugal, and pterygoid (Figs. 12–13).

IVPP V18639 consists of disarticulated but well-preserved skull elements, including a complete left jugal, partial premaxillae, and a partial right quadratojugal (Fig. 14).

IVPP V18640 consists of disarticulated, well-preserved skull elements, including the right postorbital, right jugal, caudal ramus of the left jugal, left quadrate, left quadratojugal, and both partial mandibles (Fig. 15).

IVPP V18637 is a nearly complete skull lacking a mandible (Figs. 16–18). It is the largest specimen, with a skull length (rostral to quadrate condyle) of approximately 23 cm. Both of the maxillae are damaged, and the left jugal, postorbital, and squamosal are not preserved. Both the basicranium and palate are well preserved. The postcranial skeleton is partially preserved but not fully prepared and includes seven dorsal and eight caudal vertebrae, a partial sacrum, right pelvic girdle, left femur and tibia, and left pes.

IVPP V18684 is a partial skull and nearly complete postcranial skeleton. It consists of the skull roof exposed in dorsal view and a disarticulated left maxilla, quadrate, dentary, splenial, and angular. The exoccipital, basioccipital, and basisphenoid are articulated but separate from the skull (Fig. 20). The postcranial skeleton contains two separated cervical vertebrae, articulated dorsal, sacral, and proximal caudal vertebrae, a scapula, pelvic girdle, left forelimb, and both manuses.

Locality and Horizon—As for the genus.

DESCRIPTION

General Comments

The skull is low and triangular in lateral and dorsal views (Figs. 2–4, 8, 10, 16). The skull tapers rostrally and is widest across the caudal part of the jugal, as in other basal ceratopsians (Sereno, 2000). The preorbital region is relatively short, occupying approximately 34% of the skull length.

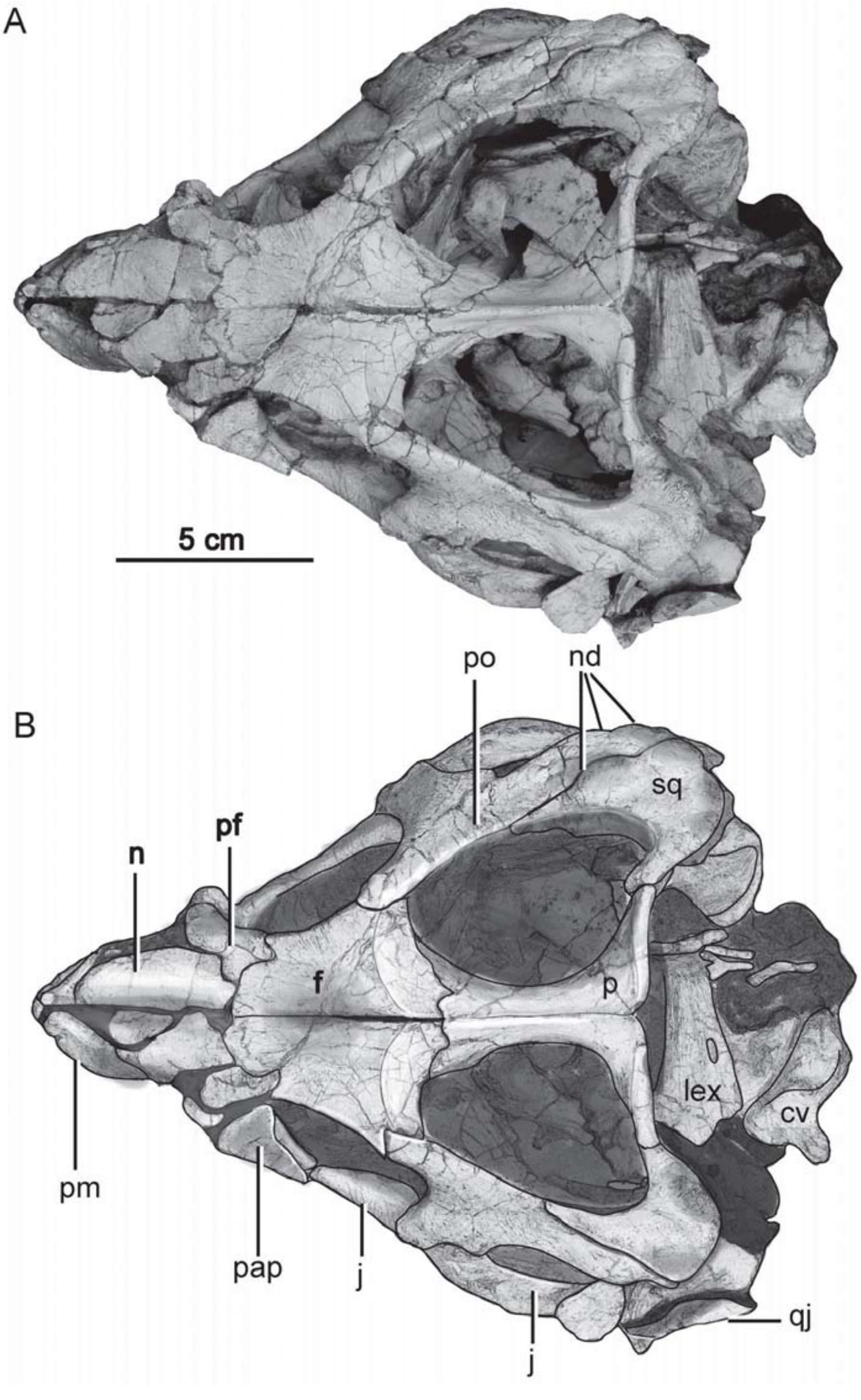

FIGURE 4. *Yinlong downsi* IVPP V14530 (holotype) skull in dorsal view. **A**, photograph; **B**, drawing. **Abbreviations**: **cv**, cervical vertebra; **f**, frontal; **j**, jugal; **lex**, left exoccipital; **n**, nasal; **nd**, nodes; **p**, parietals; **pap**, palpebral; **pf**, prefrontal; **pm**, premaxilla; **po**, postorbital; **qj**, quadratojugal; **sq**, squamosal.

The squamosals form the most caudal portion of the parietosquamosal frill, which is short and overhangs the occipital condyle only slightly. Detailed measurements of the skulls and mandibles are found in Supplemental Data (Table S1 and Fig. S1).

The orbit is circular or subcircular and smaller than the infratemporal fenestra (Figs. 2, 3). The external naris is small and elliptical, with its long axis extending caudodorsally (Figs. 2, 16). The ventral margins of the naris and infratemporal fenestra lie at the same level and slightly below the orbit. The well-circumscribed antorbital fossa is deep, subrectangular, and larger than the naris. The supratemporal fenestra is subtriangular in outline and narrows rostrally (Figs. 4, 10, 16). The height of the mandible at the coronoid process is twice the height of the dentary along the tooth row. The external mandibular fenestra, which lies at the junction of the dentary, surangular, and angular, is small and subrounded.

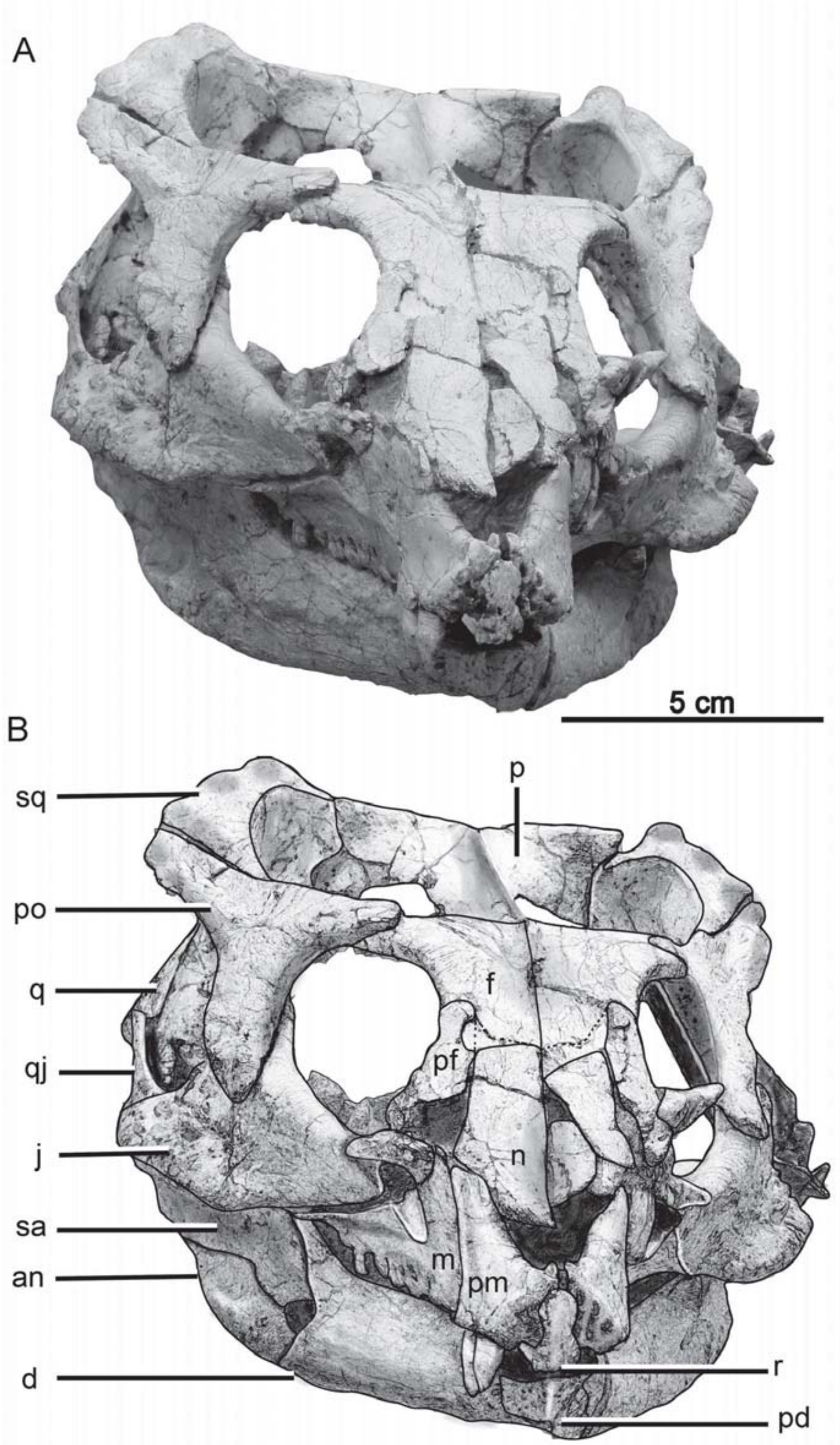

FIGURE 5. *Yinlong downsi* IVPP V14530 (holotype) skull and mandible in rostral view. **A**, photograph; **B**, drawing. **Abbreviations**: **an**, angular; **d**, dentary; **f**, frontal; **j**, jugal; **m**, maxilla; **n**, nasal; **p**, parietals; **pd**, predentary; **pf**, prefrontal; **pm**, premaxilla; **po**, postorbital; **q**, quadrate; **qj**, quadratojugal; **r**, rostral; **sa**, surangular; **sq**, squamosal.

Skull

Rostral—The rostral bone consists of a subtriangular main body that supports two buccal (lateral) processes and one dorsal process (Figs. 2–5, 8–11, 16–18). The short dorsal process overlaps the rostral surfaces of the paired premaxillae and tapers to a rounded terminus just above the ventral margin of the external naris. It neither contacts the nasal nor contributes to the external naris, as in other basal ceratopsians, but unlike *Psittacosaurus* where the rostral contacts the nasal and contributes to the narial margin (Sereno, 1990). The buccal process extends along the ventral margin of the premaxilla and terminates in front of the

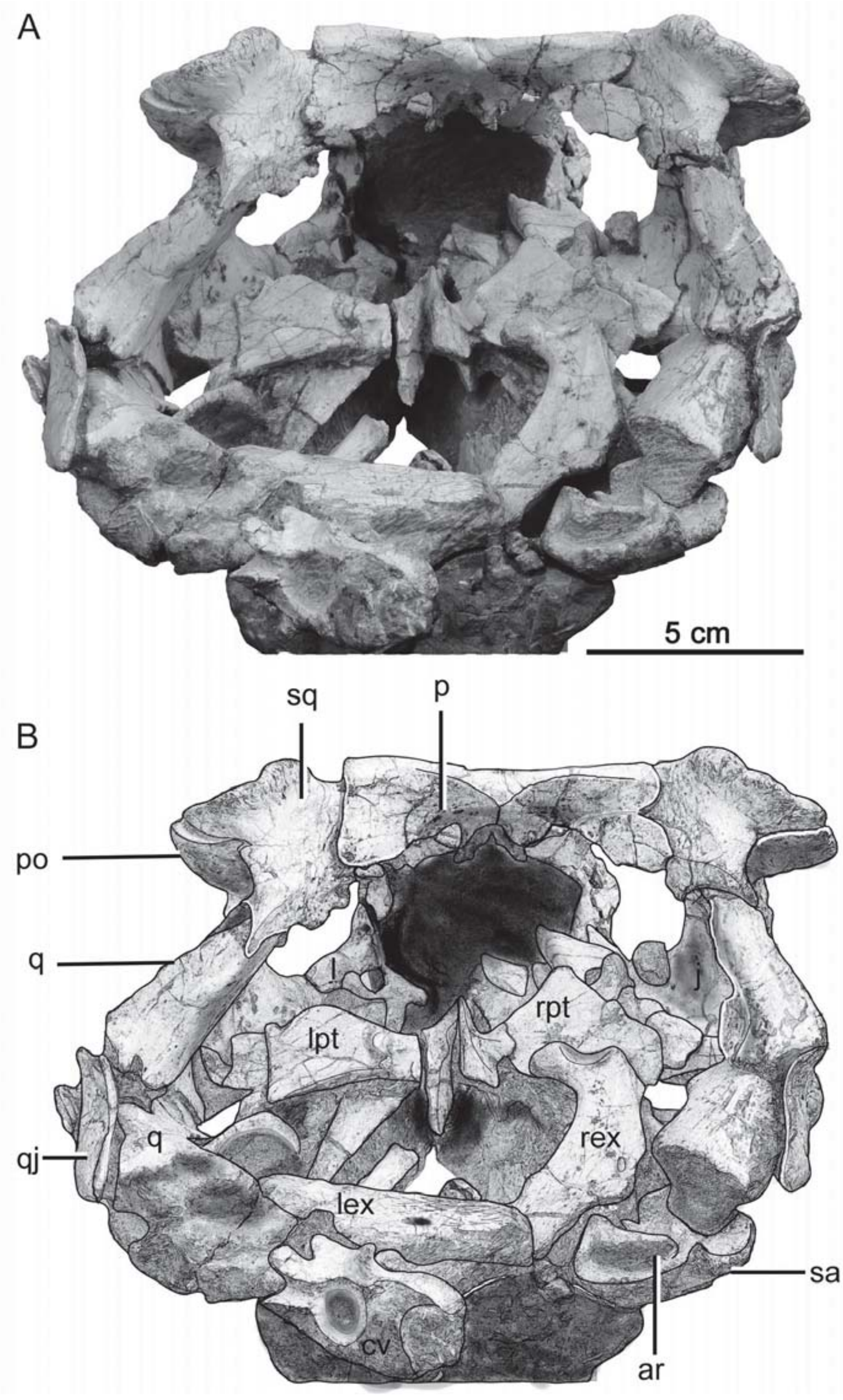

FIGURE 6. *Yinlong downsi* IVPP V14530 (holotype) skull and mandible in caudal view. **A**, photograph; **B**, drawing. **Abbreviations**: **ar**, articular; **cv**, cervical vertebra; **j**, jugal; **l**, lacrimal; **lex**, left exoccipital; **lpt**, left pterygoid; **p**, parietals; **po**, postorbital; **q**, quadrate; **qj**, quadratojugal; **rex**, right exoccipital; **rpt**, right pterygoid; **sa**, surangular; **sq**, squamosal.

first alveolus of the premaxilla, a derived character seen in neoceratopsians (Makovicky and Norell, 2006). In lateral view, the caudal margins of the main body and dorsal process form a nearly straight vertical margin. The oral margin is straight in lateral view and deflected rostroventrally approximately 30° from horizontal. This is similar to the condition in the basal neoceratopsian *Liaoceratops* (IVPP V12738) and *Psittacosaurus* (e.g., *Psittacosaurus lujiatunensis*; IVPP V12617), but differs from derived neoceratopsians, including *Archaeoceratops* and *Protoceratops*, in which the oral margin is strongly curved (Sereno, 1990; You and Dodson, 2003). In *Chaoyangsaurus* (IGCAGS V371), the rostral is deflected more ventrally than in *Yinlong* (Zhao et al., 1999; You and Dodson, 2003).

The surface of the rostral bone bears grooves and/or texture (Figs. 5, 11D) as in other ceratopsians (Makovicky and Norell, 2006). A weak midline keel is present along the lower portion of the rostral bone, as in *Chaoyangsaurus* and *Yamaceratops* (Makovicky and Norell, 2006), which differs from the sharp keel

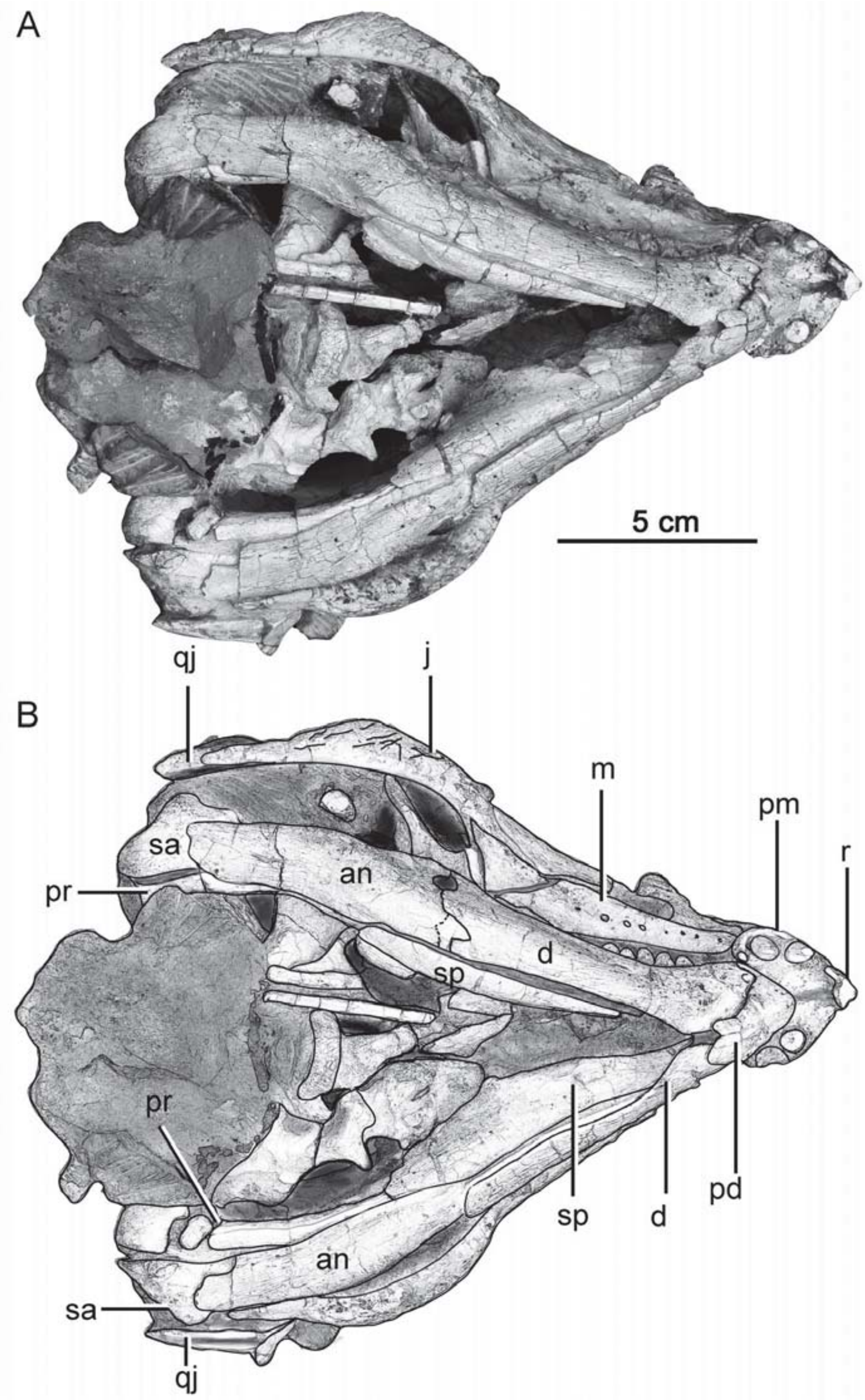

FIGURE 7. *Yinlong downsi* IVPP V14530 (holotype) skull and mandible in ventral view. **A**, photograph; **B**, drawing. **Abbreviations**: **an**, angular; **d**, dentary; **j**, jugal; **m**, maxilla; **pd**, predentary; **pm**, premaxilla; **pr**, prearticular; **qj**, quadratojugal; **r**, rostral; **sa**, surangular; **sp**, splenial.

seen in more derived neoceratopsians such as *Archaeoceratops* (You and Dodson, 2003) and *Auroraceratops* (Morschhauser, 2012). Dorsally, the rostral bone is rounded and unkeeled. In *Psittacosaurus*, the rostral lacks any keel (Sereno, 2010). The palatal surface of the rostral is slightly concave; the rostral intervenes between the premaxillae on the palatal midline for a very short distance (Fig. 18).

Premaxilla—The large premaxilla is nearly half the length of the maxilla and includes a small, rostrally positioned nasal process and a substantial caudodorsally projecting maxillary process (Figs. 2–5, 8, 11, 16–17). The main body is longer than tall, as in *Liaoceratops* and *Archaeoceratops*, but unlike *Psittacosaurus* and more derived neoceratopsians, such as *Protoceratops*, which have a relatively deep premaxilla and a dorsally placed naris (Sereno, 1990; You and Dodson, 2004). The premaxilla bears three teeth and forms the caudal, ventral, and rostral margins of the naris.

The thick main body of the premaxilla reaches its widest point adjacent to the second premaxillary tooth, as in other basal neoceratopsians, such as *Liaoceratops* (Xu et al., 2002) and

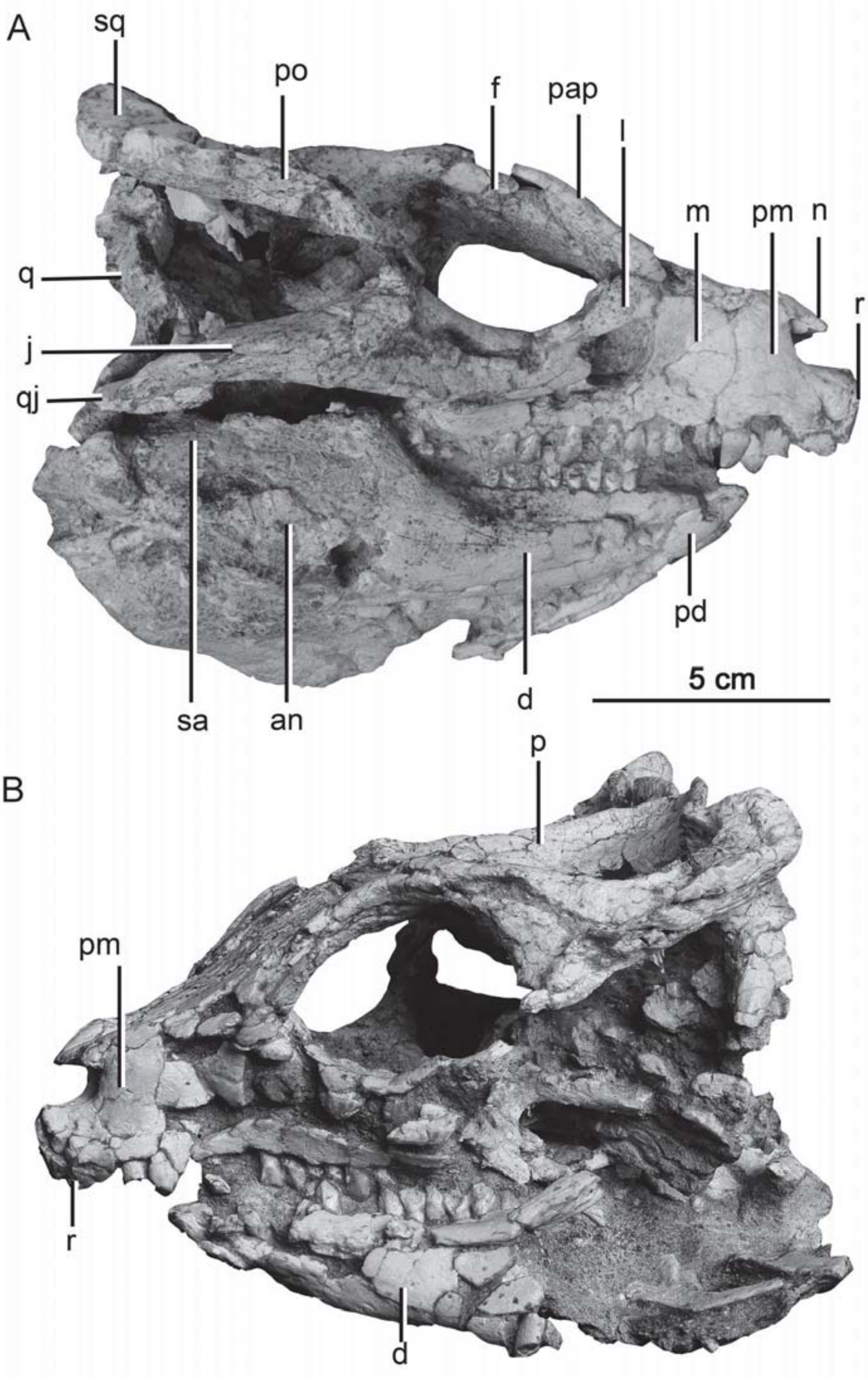

FIGURE 8. *Yinlong downsi* IVPP V18636 skull and mandible in **A**, right lateral, **B**, left lateral views. **Abbreviations**: **an**, angular; **d**, dentary; **f**, frontal; **j**, jugal; **l**, lacrimal; **m**, maxilla; **n**, nasal; **p**, parietals; **pap**, palpebral; **pd**, predentary; **pm**, premaxilla; **po**, postorbital; **q**, quadrate; **qj**, quadratojugal; **r**, rostral; **sa**, surangular; **sq**, squamosal.

Auroraceratops (Morschhauser, 2012), as well as in the basal cerapodan *Agilisaurus louderbacki* (ZDM 6011). In *Heterodontosaurus tucki*, the premaxilla reaches its widest point adjacent to the third premaxillary tooth (see Norman et al., 2011). The premaxillary body has a convex lateral surface and is notably thickened along the caudal and ventral margins of the naris, reaching at least 6 mm in IVPP V14530.

In medial view, the entire rostral and ventral portions of the premaxillae have extensive contacts with one another, resulting in a very thick primary palate and a substantial substrate for the rostral bone (Fig. 5A). The joined premaxillae form a shallow midline sulcus along their rostral margin for the reception of the rostral bone. The surface of the premaxilla is mediolaterally thickened, flat, and angled rostrolaterally where it underlies the rostral bone. The lateral surface of the premaxilla is rugose and bears several deep pits immediately behind the rostral bone (IVPP V14530). Above this, the nasal processes form the rostral and rostrodorsal margins of the nares and intercede between the nasals for a short distance.

On the lateral surface, the premaxilla-maxilla suture runs rostrodorsally up from the oral margin before turning sharply caudodorsally along the rear of the maxillary process, approximately at

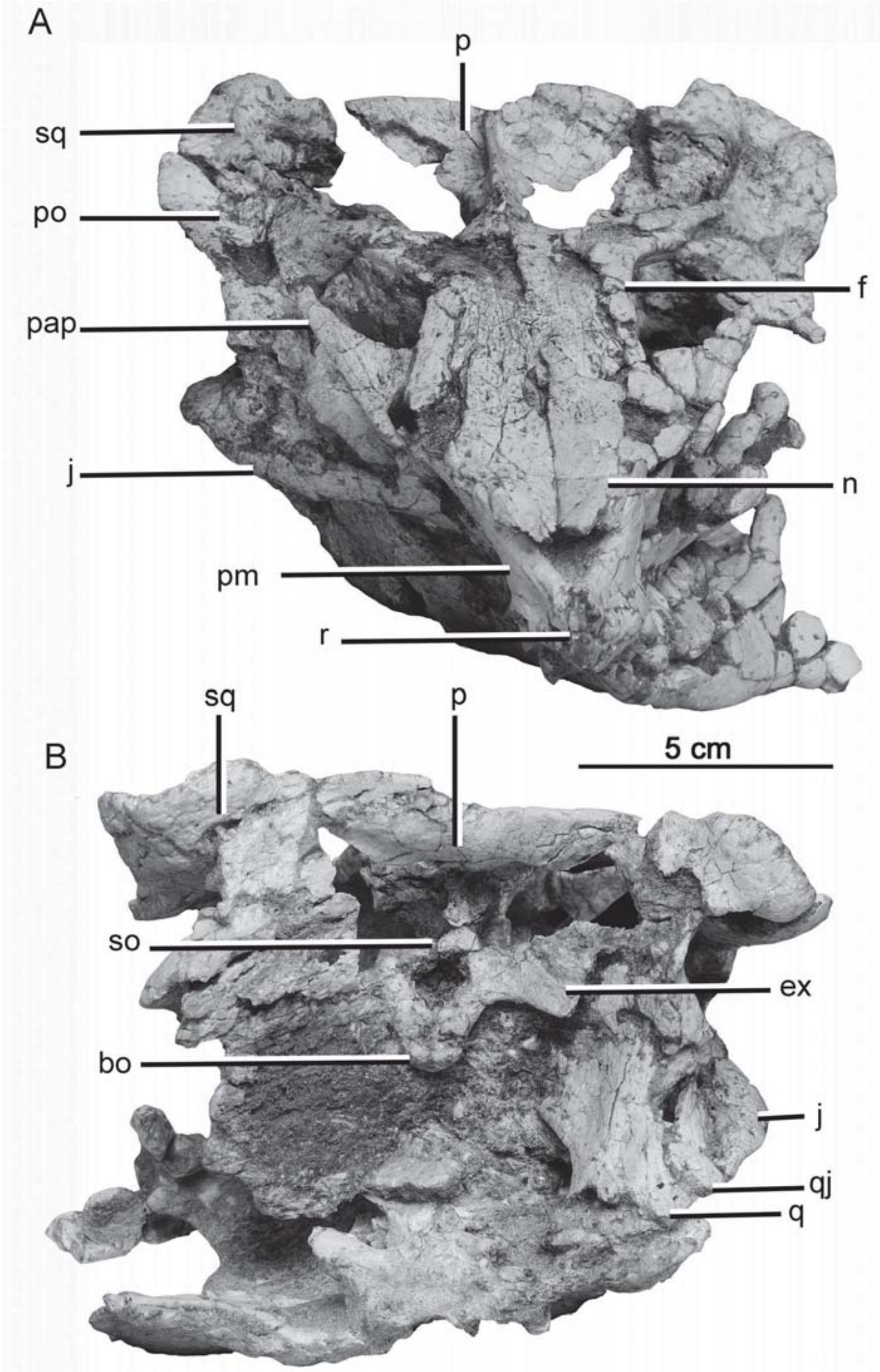

FIGURE 9. *Yinlong downsi* IVPP V18636 skull and mandible in **A**, rostral, **B**, caudal views. **Abbreviations**: **bo**, basioccipital; **ex**, exoccipital; **f**, frontal; **j**, jugal; **n**, nasal; **p**, parietals; **pap**, palpebral; **pm**, premaxilla; **po**, postorbital; **q**, quadrate; **qj**, quadratojugal; **r**, rostral; **so**, supraoccipital; **sq**, squamosal.

the level of the ventral narial margin. A similarly angled suture also occurs in *Auroraceratops* (Morschhauser, 2012) and some basal ornithopods such as *Jeholosaurus* (IVPP V15716; Barrett and Han, 2009), whereas a more vertical suture is present in the basal ceratopsians *Liaoceratops* (IVPP V12633, IVPP V12738) and *Archaeoceratops* (IVPP V11114). The broad maxillary process is much wider than the nasal processes in lateral view. It extends caudodorsally about 20° from vertical and forms the caudal margin of the naris. Its rostral and caudal margins are nearly parallel, and the process terminates in an angled suture with the nasal. This feature differs from *Psittacosaurus*, which has a much broader process, and basal ornithopods and *Heterodontosaurus*, which have long, tapering processes (Barrett and Han, 2009; Norman et al., 2011). The maxillary process is separated from the lacrimal by the maxilla, as in *Liaoceratops* (IVPP V12633: Xu et al., 2002), whereas the premaxilla and lacrimal contact in derived ceratopsians such as *Archaeoceratops* (contra You et al., 2003) and *Auroraceratops*. In lateral view, the maxillary process does not extend beyond the caudal margin of the main body, as in *Auroraceratops* (Morschhauser, 2012) and *Leptoceratops*

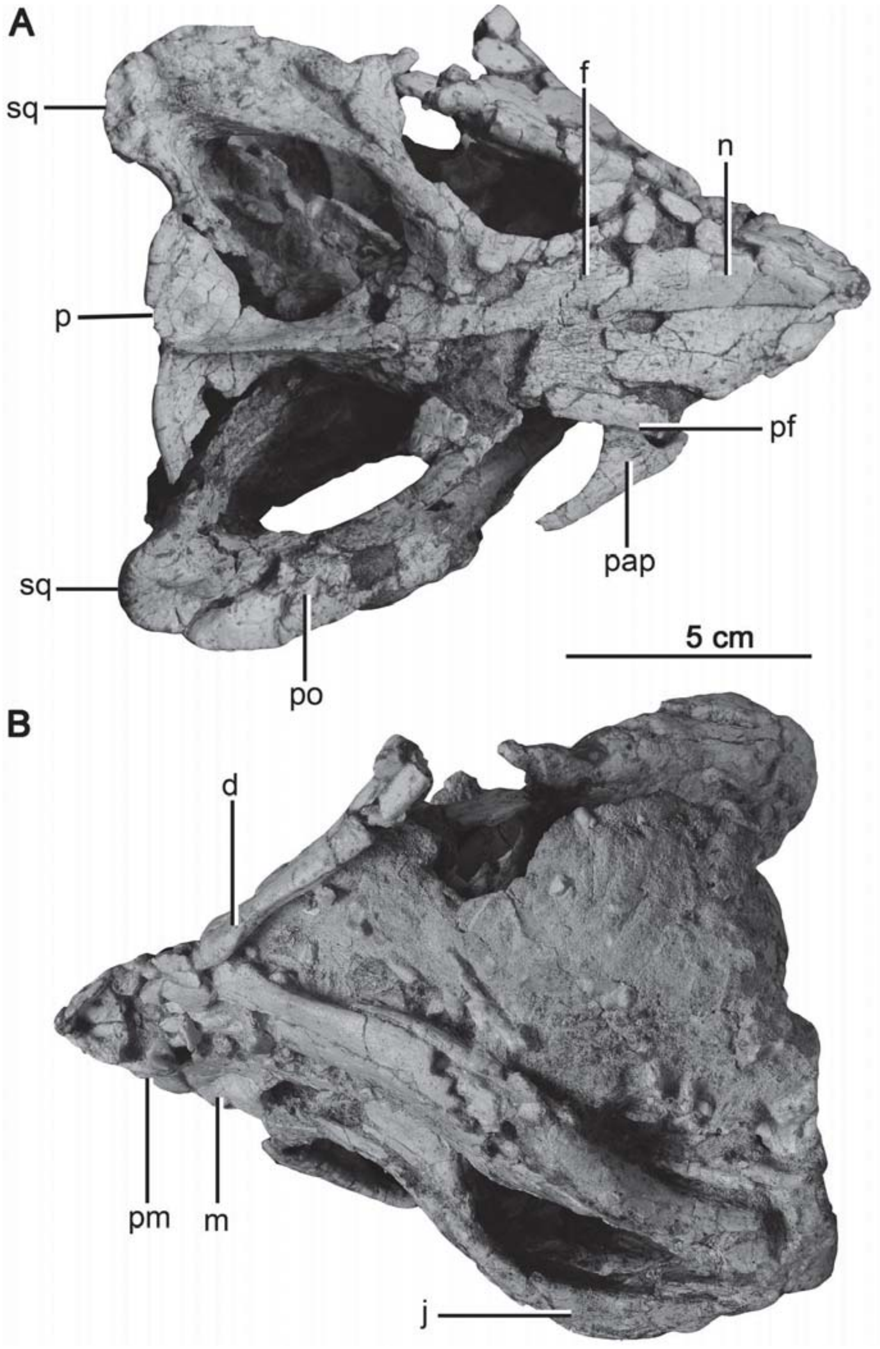

FIGURE 10. *Yinlong downsi* IVPP V18636 skull and mandible in **A**, dorsal, **B**, ventral views. **Abbreviations**: **d**, dentary; **f**, frontal; **j**, jugal; **m**, maxilla; **n**, nasal; **p**, parietals; **pap**, palpebral; **pf**, prefrontal; **pm**, premaxilla; **po**, postorbital; **sq**, squamosal.

(Sternberg, 1951), but unlike *Liaoceratops* (Xu et al., 2002) where the maxillary process extends further caudally. The medial surface of the maxillary process is thick where it faces the naris, but bears a deep fossa along most of its caudal portion.

The premaxillae have an extensive palatal contact, extending as far back as the rear of the first premaxillary tooth, and are broadly vaulted across the midline, as in other ceratopsians (Sereno, 2000). A fossa is present in the rostral region of the premaxillary palate (IVPP V18636, IVPP V18637), as in *Liaoceratops* (IVPP V12633, IVPP V12738) and *Archaeoceratops* (IVPP V11114). The diamond-shaped rostral part of the vomers underlies and intercedes a short distance between the premaxillae at the rear of the premaxillary palate. On the caudal surface of the premaxilla, immediately above the oral margin and within its thickened palatal portion, is a deep socket for the reception of a rostral process (peg) of the maxilla.

Three teeth are present in the premaxilla, as in other basal ceratopsians such as *Liaoceratops* (Xu et al., 2002), *Archaeoceratops* (You and Dodson, 2003), and *Auroraceratops* (You et al., 2005), in pachycephalosaurs (Maryańska et al., 2004), and in *Heterodontosaurus* (Norman et al., 2011). However, there are only two premaxillary teeth in *Chaoyangsaurus* (Zhao et al., 1999) and *Protoceratops andrewsi* (Brown and Schlaijker, 1940) and just one in *Xuanhuaceratops* (Zhao et al., 2006).

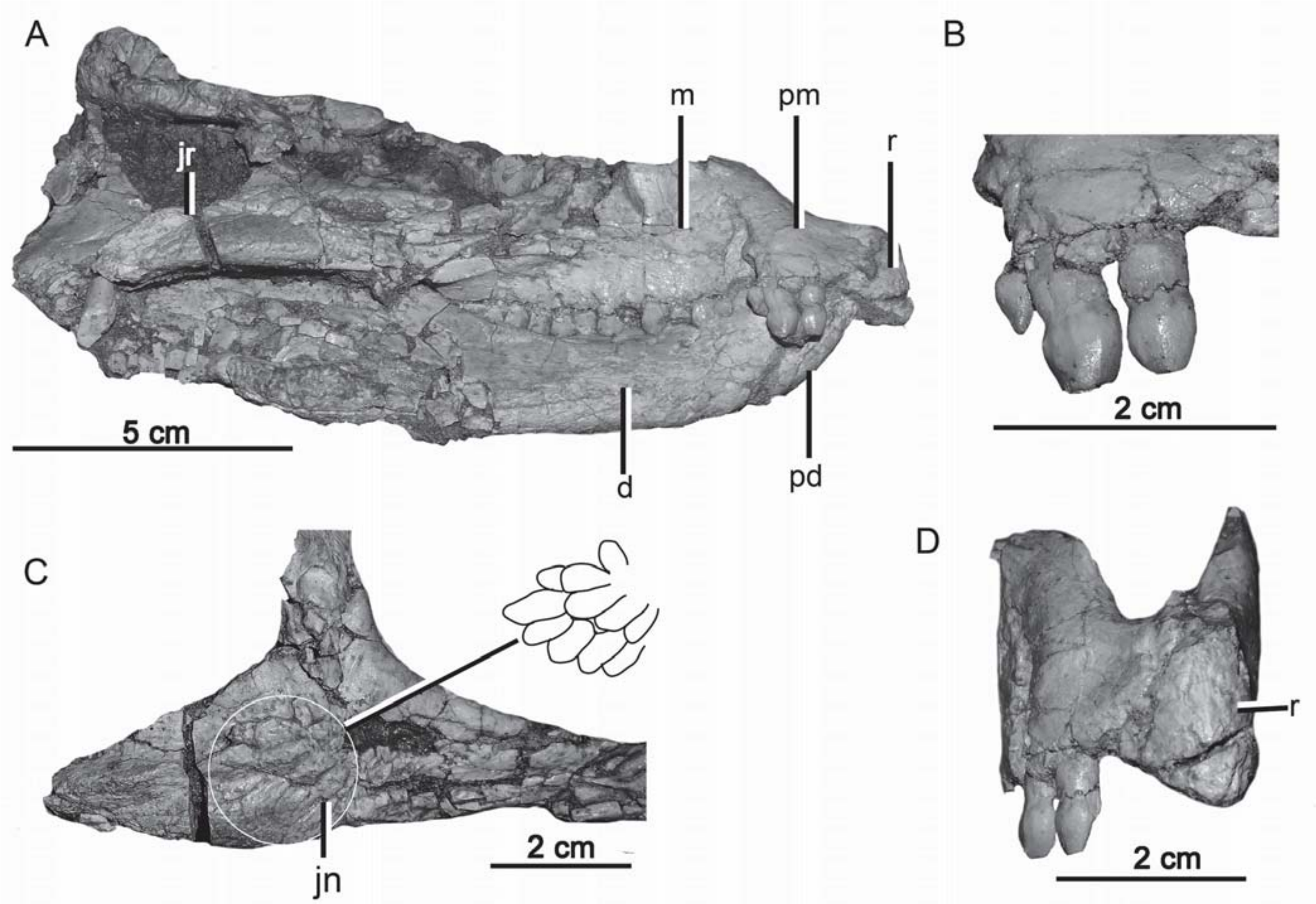

FIGURE 11. *Yinlong downsi* IVPP V18686 skull and mandible. **A**, skull and mandible in right lateral view; **B**, premaxillary teeth in right lateral view; **C**, jugal in right lateral view, line drawing of nodes; **D**, rostral and premaxilla in rostral view. **Abbreviations**: **jn**, jugal nodes; **jr**, jugal ridge; **m**, maxilla; **pm**, premaxilla; **r**, rostral.

Premaxillary teeth are absent in *Psittacosaurus* (Sereno, 1990) and *Leptoceratops* (Sternberg, 1951). Three premaxillary teeth may represent a synapomorphy of marginocephalians and heterodontosaurids (Norman et al., 2011).

Maxilla—The maxilla is twice as long as it is high (Figs. 2–4, 8, 11–13, 16–18, 20). The tooth row is medially inset to form a buccal emargination, although not as deeply as in other ceratopsians. The buccal emargination is very weak rostrally and occurs relatively high on the maxilla, just below the level of the antorbital fossa.

There are 13 maxillary teeth in *Yinlong* (IVPP V14530, IVPP V18638, and IVPP V18684, Figs. 2, 12, 20), as in *Archaeoceratops* (IVPP V11114) and *Liaoceratops* (IVPP V12738). There are 12 maxillary teeth in *Auroraceratops* (Morschhauser, 2012), 11 or 12 maxillary teeth in *Yamaceratops* (Makovicky and Norell, 2006), eight to 12 maxillary teeth in adult *Psittacosaurus* (Sereno, 1990), and nine maxillary teeth in *Chaoyangsaurus*. Higher maxillary tooth counts occur in *Protoceratops* and *Leptoceratops* (You and Dodson, 2004). The first maxillary tooth begins immediately behind the premaxillary suture, eliminating any diastema. In ventral view, the maxillary tooth rows approach each other rostrally so that the first maxillary tooth lies closer to the midline than does the third premaxillary tooth, as in other ceratopsians (e.g., *Liaoceratops, Archaeoceratops*). The maxillary and premaxillary oral margins occur at the same level. Nine foramina are arranged just below the line of emargination in the maxilla. These foramina become progressively larger caudally (IVPP V14530) but do not reach to the most caudal tooth position. The tooth row extends to the rear of the maxilla and is fully exposed in lateral view when the mandible is articulated.

The maxilla has an angled suture with the premaxilla, as described above. Extending rostrally, immediately above the first maxillary tooth, is a blunt rostral process (peg) that inserts into a deep socket in the rear of the premaxilla (Fig. 13). This process is centered 10 mm above the oral margin and extends 11 mm in front of the tooth row in IVPP V18638; it is covered in lateral view when the premaxilla is articulated. The medial aspect of the articular peg extends medial to the body of the maxilla; its surface is striated for articulation with either the vomer or contralateral maxilla. In ventral view, the rostral maxillae do not appear to contact, although it is possible that such a contact occurs deep to the vomer.

Immediately above the articular peg is a deep sulcus that runs rostrocaudally across the front half of the medial side of the maxilla (Fig. 13). A large foramen pierces the floor of this sulcus. When articulated, the rostral end of this sulcus meets the base of the fossa on the medial surface of the maxillary process of the premaxilla.

The maxilla appears to have a very short contact with the nasal in IVPP V18637. The maxilla has a long caudoventrally directed suture with the lacrimal. A deep subrectangular antorbital fossa, which narrows caudally, is present on the maxilla. This differs from the neoceratopsians *Liaoceratops*

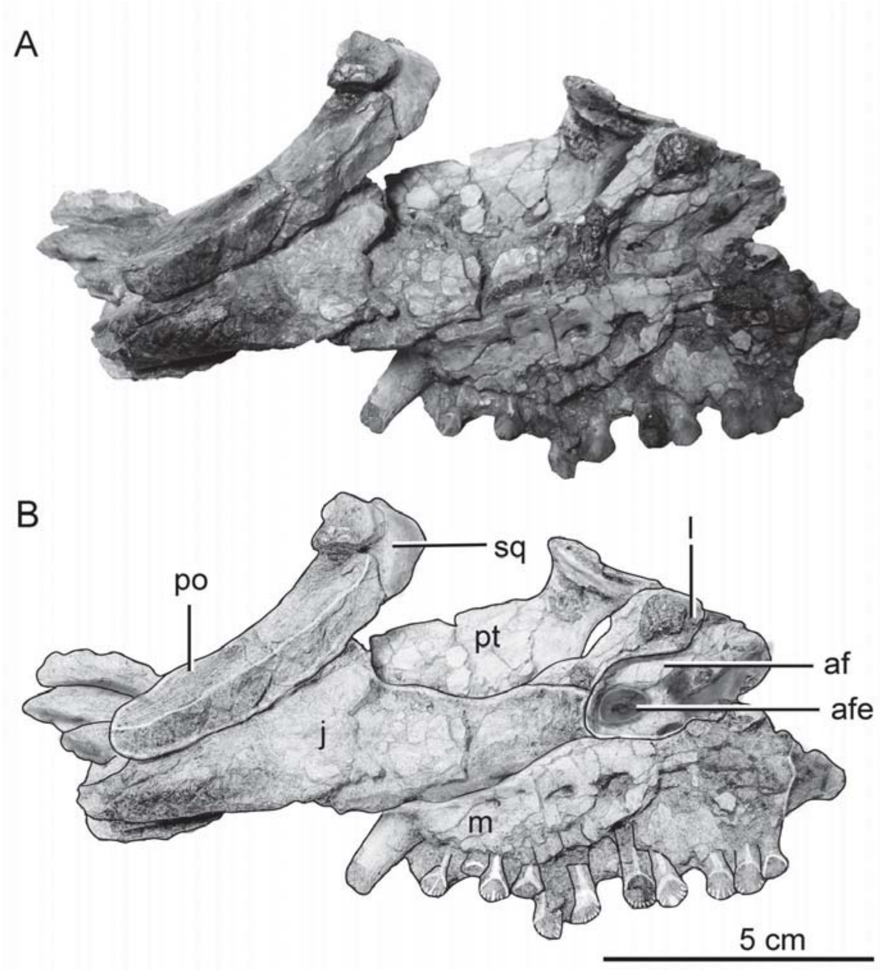

FIGURE 12. *Yinlong downsi* IVPP V18638 right side of partial skull in lateral view. **A**, photograph; **B**, drawing. **Abbreviations**: **af**, antorbital fossa; **afe**, antorbital fenestra; **j**, jugal; **l**, lacrimal; **m**, maxilla; **po**, postorbital; **pt**, pterygoid; **sq**, squamosal.

(IVPP V12633) and *Archaeoceratops*, which have a subtriangular fossa (Xu et al., 2002; You and Dodson, 2003). All margins of the antorbital fossa are prominent, unlike other neoceratopsians, where the rostral margin is weakly defined (e.g., *Liaoceratops*) or absent (*Archaeoceratops*; You and Dodson, 2003). Both the dorsal and ventral portions of the antorbital fossa are invaginated beneath their margins. The rostral and ventral margins of the fossa are formed by the maxilla, the dorsal margin by the lacrimal, and the short caudal margin by the jugal. The inner wall of the antorbital fossa is formed primarily by the maxilla, with a small contribution by the lacrimal. A large, oval antorbital fenestra pierces the maxilla on the caudodorsal floor of the antorbital fossa, opening rostrolaterally, as also occurs in other basal neoceratopsians such as *Liaoceratops* (Xu et al., 2002) and *Archaeoceratops* (You and Dodson, 2003).

Behind the antorbital fossa, the maxilla and jugal have a long, straight, caudoventrally directed suture. The lateral surface of the maxilla forms a substantial thickened buttress to support the jugal; it also forms the dorsal boundary of the cheek emargination (Figs. 2, 3). Behind this, the maxilla splits into caudally directed lateral and medial processes. The more lateral of these processes extends dorsolaterally to underlie the jugal. The other process angles slightly medially to contact the ectopterygoid. A well-defined embayment separates these two processes.

Nasal—The broad nasal narrows both rostrally and caudally, and the roof of the nasal is slightly arched (Figs. 2–5, 9, 10, 16). The paired nasals join in a straight midline suture and have a well-developed longitudinal fossa along their junction. Nasal fossae occur in the basal ceratopsian *Liaoceratops* (Xu et al., 2002), the basal ornithischians *Heterodontosaurus* (Norman et al., 2011) and *Agilisaurus* (Peng, 1992), and the basal ornithopods *Jeholosaurus* (Xu et al., 2000; Barrett and Han, 2009) and *Changchunsaurus* (Jin et al., 2010).

The nasals tapers rostrally to envelop the nasal processes of the premaxillae. The nasal forms the caudodorsal margin of the external naris, unlike the situation in *Psittacosaurus*, in which the nasal forms the entire dorsal half of the external naris (Sereno, 1990). Behind the nares, the nasal has a long, caudodorsally directed suture with the dorsal margin of the maxillary process of the premaxilla. In IVPP V18686, the rostral part of the nasal has a concave articular facet that receives the premaxilla. A rugose ridge occurs at this contact and continues caudally along the prefrontal. This ridge marks the change in slope between the dorsum and side of the snout, as in other basal ornithischians (e.g., *Jeholosaurus*). The nasal has a short contact with the maxilla (IVPP V18637), then an extensive, sinuous contact with the prefrontal. The nasals reach their maximum width at the rostral end of the prefrontal, then narrow towards the frontals. They have a broad overlapping suture with the rostral surface of the frontal, although the frontals briefly intervene between the nasals on the midline (Figs. 4, 5).

Lacrimal—The lacrimal is a subtriangular element that forms the rostroventral margin of the orbit and the caudodorsal portion of the antorbital fossa (Figs. 2, 3, 8, 12). Where it forms the

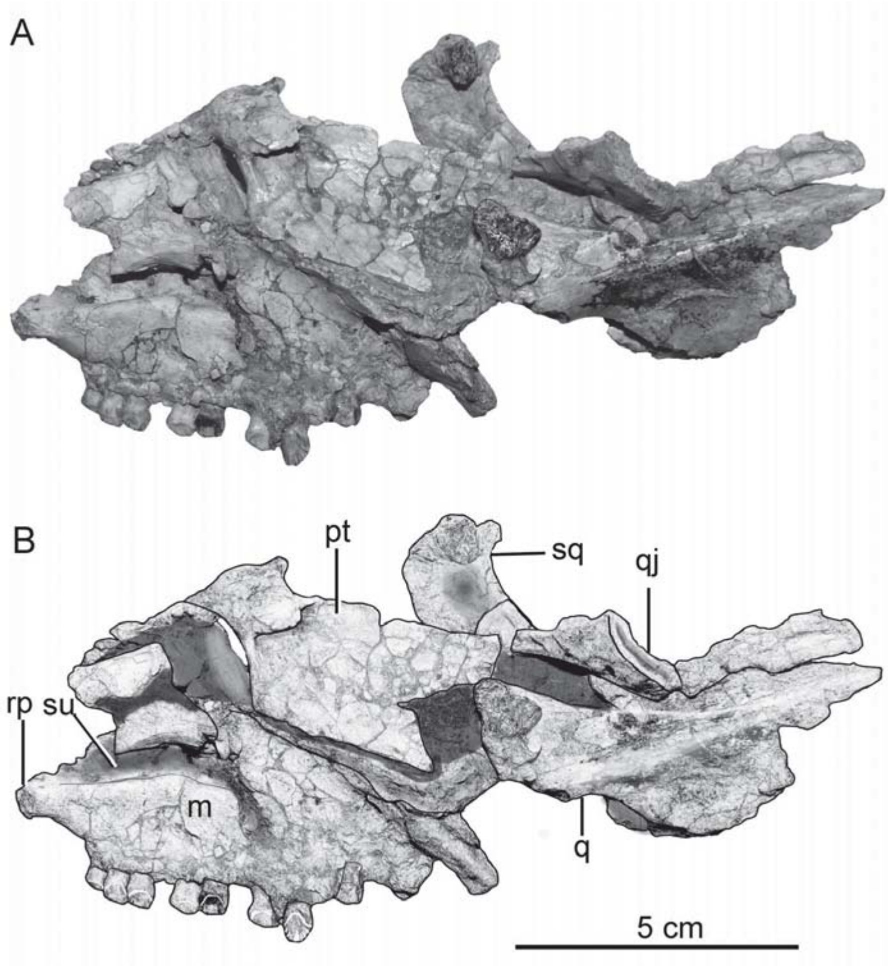

FIGURE 13. *Yinlong downsi* IVPP V18638 right side of partial skull in medial view. **A**, photograph; **B**, drawing. **Abbreviations**: **m**, maxilla; **pt**, pterygoid; **q**, quadrate; **qj**, quadratojugal; **rp**, rostral process; **sq**, squamosal; **su**, sulcus on the maxilla.

orbital margin, the lacrimal is mediolaterally thickened dorsally, but narrows to the jugal contact. A prominent fossa is present near the mid-portion of the lacrimal (Fig. 3), as in *Psittacosaurus* (Sereno, 1987), *Archaeoceratops*, and *Liaoceratops*, although it is very weak in the latter two genera (pers. observ.).

The lacrimal forms a short scarf joint with the jugal that extends caudodorsally from the antorbital fossa. The lacrimal meets the maxilla rostroventrally along the floor of the antorbital fossa. Its dorsal margin has a substantial, nearly horizontal suture with the prefrontal. The lacrimal does not contact the nasal, as in the basal neoceratopsians *Liaoceratops* (Xu et al., 2002), *Archaeoceratops*, and *Heterodontosaurus* (contra You and Dodson, 2003), but unlike *Auroraceratops* (Morschhauser, 2012) and other derived neoceratopsians (You and Dodson, 2004) where these elements make contact.

Prefrontal—The prefrontal forms the rostrodorsal margin of the orbit and articulates with the palpebral (Figs. 3–5, 9–10). In lateral view, the prefrontal is ‘L’-shaped, with a ventral ramus that forms the rostral margin of the orbit and a caudal ramus that forms the rostrodorsal margin of the orbit.

The prefrontal has a long, sinuous contact with the nasal medially. Caudally, the prefrontal narrows to a blunt point that inserts into a small embayment on the rostrolateral edge of the frontal, so that the frontal has a short orbital margin lateral to the prefrontal (Fig. 4A). Rostrally, the prefrontal has a short contact with the maxilla, then a longer, nearly horizontal suture with the dorsal margin of the lacrimal. The orbital margin of the prefrontal is well defined and mediolaterally thickened to form a base for articulation with the palpebral. The wedge-shaped ventral ramus tapers caudoventrally, forming a right angle with the more dorsal part of the element, as in *Yamaceratops* (Makovicky and Norell, 2006) and *Archaeoceratops* (pers. observ.).

Palpebral—The palpebral is an elongate, rod-like element that consists of short rostral and dorsal articular processes and a longer orbital process (Figs. 3, 4, 8–10; in IVPP V14530, the palpebral on the left side is actually the right palpebral). The orbital process reaches approximately half way across the orbit and is located approximately one-third of the way down the orbit. It is slender along its length, slightly curved dorsally at its distal end, and tapers to a blunt point. The rostral articular process extends across the lateral face of the prefrontal, in line with the orbital process. It gently expands dorsomedially and has a subtriangular cross-section. The medial surface is flat and slightly rugose for articulation with the prefrontal. The dorsal articular process is rostrocaudally wide, dorsoventrally compressed, and tapered distally. The entire dorsal process curves caudodorsally to follow the orbital margin. The dorsal process is depressed relative to the orbital and rostral processes, as in other basal ornithischians (e.g., *Agilisaurus*), but unlike the situation in other basal neoceratopsians (e.g., *Archaeoceratops, Psittacosaurus*) where these processes are confluent.

Frontal—The broad, elongate frontals form the majority of the skull roof and the entire dorsal margin of the orbits (Figs. 2–5, 8–10, 16, 17). The paired frontals connect with each other in a

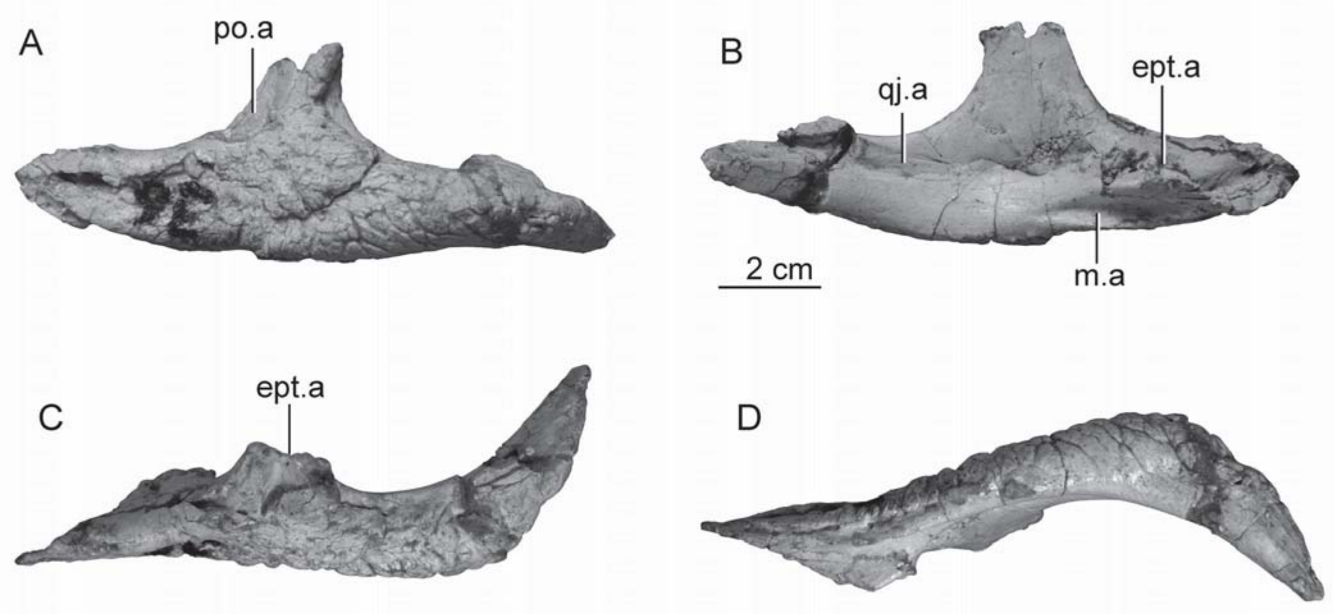

FIGURE 14. *Yinlong downsi* IVPP V18639 left jugal in **A**, lateral, **B**, medial, **C**, dorsal, **D**, ventral views. **Abbreviations**: **ept.a**, articular surface for ectopterygoid; **m.a**, articular surface for maxilla; **po.a**, articular surface for postorbital; **qj.a**, articular surface for quadratojugal.

straight line, which is indented by a shallow midsagittal depression. This depression is weak in the smallest specimen (IVPP V18636) but prominent in the holotype (IVPP V14530) and IVPP V18637 (Figs. 4, 10, 16); it is restricted to the rostral region of the paired frontals in IVPP V14530 but extends nearly the entire length of the frontals in IVPP V18637. This feature is identified as an autapomorphy of *Yinlong* (Xu et al., 2006). The ventral surface of the frontals below this depression is excavated for the olfactory tract. This excavation is wide and shallow rostrally, narrows at mid-length, then widens towards the braincase, as in other ornithischians (e.g., *Liaoceratops, Archaeoceratops, Psittacosaurus*; Sereno, 2010). The frontal depressions thus demarcate an area of thinned frontal bone.

The frontal reaches its greatest width at the postorbital process and narrows rostrally towards its contact with the nasals and prefrontals. The interorbital width is thus much narrower rostrally than caudally, resulting in the plane of the orbits facing forward approximately 30–35° off the sagittal plane. Many small ridges and grooves extend rostrolaterally along the orbital margin of the frontal (IVPP V14530). The frontals are broadly overlapped by the nasal medially and meet the prefrontals laterally. The frontal has a shallow socket adjacent to the orbital margin to receive the blunt caudal end of the prefrontal.

The postorbital process extends ventrolaterally at the rear of the orbit. The frontal-postorbital suture is complex, with the frontal process of the postorbital fitting firmly into a caudolaterally directed embayment on the frontal. This sinuous junction may represent a plesiomorphic character state for ornithischians (Makovicky and Norell, 2006). The ventral surface of the postorbital process of the frontals is excavated by a large fossa for articulation with the laterosphenoid.

The frontals extend a short distance behind the postorbital processes to meet the rostral parietals in a broad suture. The caudal margin of the frontals forms an irregular, complex peg-and-socket joint with the parietals. This differs from *Liaoceratops*, where the caudal margin of the frontals overlaps the parietals. The caudal margin of the frontals has a gentle emargination (Figs. 4, 10, 16), demarcating the rostral attachment of jaw adductor musculature (You and Dodson, 2004), as in many basal ceratopsians (Makovicky and Norell, 2006) and *Heterodontosaurus* (Norman et al., 2011). The frontal intervenes broadly between the parietals and postorbital along the rostral margin of the supratemporal fenestra.

The entire rear of the frontal is impressed with the arched, well-defined rostral rim of the supratemporal fossa, Laterally, the rim of the supratemporal fossa terminates at the center of the postorbital process of the frontal such that the postorbital meets the rostral margin of the supratemporal fenestrae but does not participate in it. The frontal within the fossa is very thin. The left and right supratemporal fenestrae meet on the midline, forming a short, low midline crest confluent with that on the parietals.

Postorbital—The postorbital is 'T'-shaped with constricted frontal, squamosal, and jugal processes (Figs. 2–5, 8–10, 16), similar to *Psittacosaurus* (e.g., *P. lujiatunensis*) and basal ornithischians (e.g., *Jeholosaurus, Hypsilophodon*), but unlike *Liaoceratops* and other neoceratopsians, in which the postorbital is triangular with less distinct rami (Xu et al., 2002). The frontal process is shorter than the jugal process, and the squamosal process is the longest. The postorbital forms large portions of the orbit and temporal fenestra margins.

The body of the postorbital has a flat to slightly concave lateral surface. Most of this surface is strongly rugose, with low nodular ornamentation, including two to three large marginal nodes (the last borne partially on the squamosal). This occurs in the basal ceratopsians *Archaeoceratops* (You and Dodson, 2003) and *Auroraceratops* (Morschhauser, 2012), pachycephalosaurs (Sullivan, 2006), and some basal ornithopods (e.g., *Jeholosaurus*; Barrett and Han, 2009).

The frontal process is slender and forms the caudodorsal margin of the orbit. Its surface is rounded laterally and flattened medially. Rostrally, the process slightly expands where it overlaps a facet on the postorbital process of the frontal. It is finely striated along the orbit margin. The frontal and squamosal processes together form the rostral two-thirds of the lateral margin of the supratemporal fenestra. The squamosal process is long

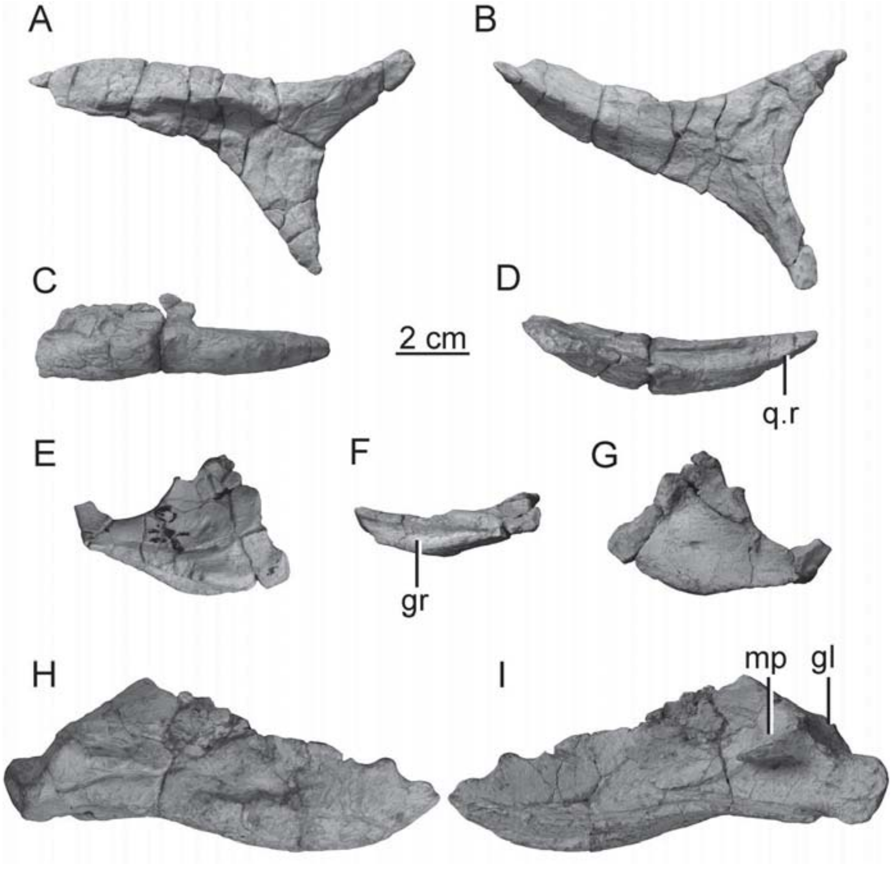

FIGURE 15. *Yinlong downsi* IVPP V18640 right postorbital in **A**, lateral, **B**, medial views; partial right jugal in **C**, lateral, **D**, dorsal views; right quadratojugal in **E**, lateral, **F**, ventral, **G**, medial views; angular and partial right surangular in **H**, lateral, **I**, medial views. **Abbreviations**: **gr**, groove articulating with jugal; **gl**, glenoid fossa; **mp**, medial process; **q.r**, ridge articulating with quadratojugal.

and narrow, forming a straight caudolaterally directed contact with the entire lateral margin of the squamosal. The extensive facet for the squamosal faces dorsomedially, unlike in other basal ceratopsians, such as *Liaoceratops* and *Archaeoceratops*, where it faces medially. The squamosal process tapers dorsoventrally and expands mediolaterally to a blunt terminus (Figs. 2, 3, 15). This is similar to *Psittacosaurus*, but quite different from the bifurcated connection with the squamosal in *Liaoceratops* (Xu et al., 2002), *Yamaceratops* (Makovicky and Norell, 2006), and *Auroraceratops* (Morschhauser, 2012). The squamosal process terminates dorsal to the quadrate cotylus of the squamosal and forms the entire dorsal margin of the infratemporal fenestra.

The jugal process is relatively wide and extends rostroventrally along the caudal margin of the orbit to meet the jugal. The lateral surface is convex, with sharp margins both rostrally and caudally, and the medial surface is flattened. A ridge extends along its entire caudal aspect on the right side of the holotype (IVPP V14530; Fig. 2). This ridge was suggested to be similar to that of *Heterodontosaurus* (Xu et al., 2006), although in the latter taxon the ridge is more prominent and extends along both the jugal and squamosal rami of the postorbital (Norman et al., 2011). The ridge does not occur on the left side of the holotype or in any other specimens and thus may represent individual variation. The jugal process of the postorbital overlaps the rostrolateral side of the postorbital process of the jugal for its entire distance. They both contribute to the postorbital bar, although in lateral view the postorbital forms the orbital margin, whereas the jugal forms the rostral margin of the infratemporal fenestra. The jugal process of the postorbital ends in a blunt tip that fits into a deep, 'V'-shaped socket in the lateral surface of the jugal.

Jugal—The large, robust jugal is strongly bowed laterally and has maxillary, postorbital, and quadratojugal processes (Figs. 2–5, 8–16, 18). The lateral excursion of the jugal makes it the widest part of the skull, as in all basal ceratopsians. Although the lower margin of the jugal is slightly convex, there is no development of a jugal flange or jugal horn, unlike other neoceratopsians and *Psittacosaurus*.

The maxillary and postorbital processes are subequal in length, and the quadratojugal process is twice the length of the maxillary process, as in *Chaoyangsaurus* (Zhao et al., 1999) and *Psittacosaurus* (e.g., *P. lujiatunensis*, IVPP V12617). The maxillary process is dorsoventrally deeper than the quadratojugal process at its base, as seen in other basal neoceratopsians except *Liaoceratops* and *Yamaceratops* (Sereno, 2000; Xu et al., 2002; Makovicky and Norell, 2006). Rugose sculpturing and/or nodular ornamentation are present on the lateral and ventral surfaces of the main body and quadratojugal process. This feature is common in other basal ceratopsians such as *Chaoyangsaurus, Xuanhuaceratops* (Zhao et al., 2006), *Archaeoceratops* (You and Dodson, 2003), and *Auroraceratops* (Morschhauser, 2012). Nodular ornamentation is also present in pachycephalosaurians (Maryańska et al., 2004) and the basal ornithopod *Jeholosaurus* (Barrett and Han, 2009). However, the ornamentation in ceratopsians is grooved and textured, whereas it is smooth in pachycephalosaurs and *Jeholosaurus*, although recent phylogenetic analyses considered them to be the same character state (Butler et al., 2008). Additionally, larger oval nodules are clustered on the jugal body (Fig. 11C) and may represent an autapomorphy of Ceratopsia.

The maxillary process of the jugal has a flattened lateral surface and tapers rostrally to meet the lacrimal and maxilla. It contacts the maxilla along a long, slightly curved suture that terminates at the antorbital fossa, where the jugal forms its short caudal margin. Above this, the maxillary process has a short, nearly horizontal suture with the lacrimal. The jugal forms the thin, mediolaterally compressed margin of the caudoventral

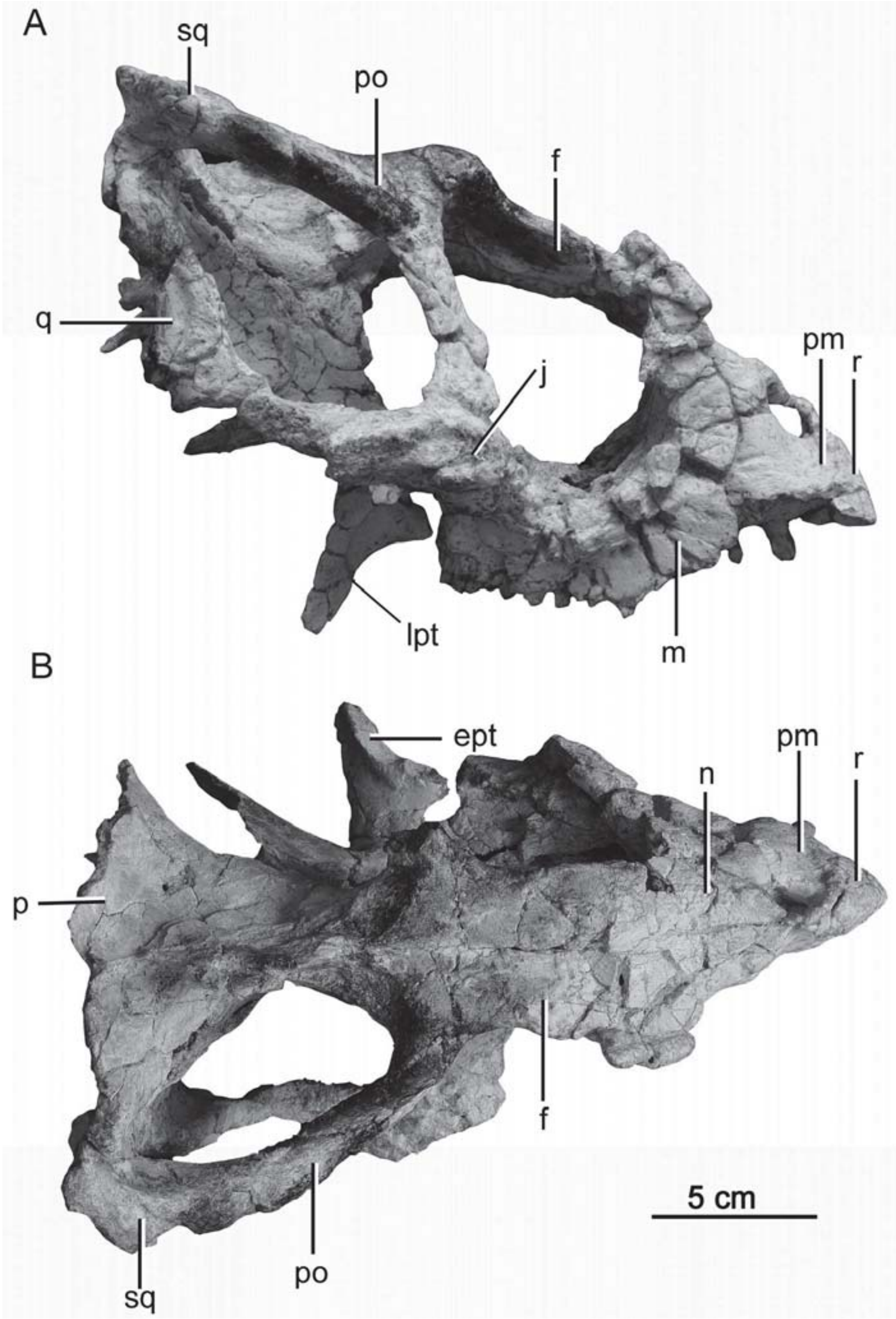

FIGURE 16. *Yinlong downsi* IVPP V18637 skull in **A**, left lateral, **B**, dorsal views. **Abbreviations**: **ept**, ectopterygoid, **f**, frontal; **j**, jugal; **lpt**, left pterygoid; **m**, maxilla; **n**, nasal; **p**, parietals; **pm**, premaxilla; **po**, postorbital; **q**, quadrate; **r**, rostral; **sq**, squamosal.

orbit. On its medial surface, the base of the maxillary process bears a rostrocaudally elongate, raised facet for articulation with the ectopterygoid. A prominent sulcus beneath this ectopterygoid facet articulates with the maxilla (Fig. 14B–D).

Most of the rostral portion of the postorbital process of the jugal is covered by the postorbital in lateral view. Where exposed, its lateral surface is convex rostrocaudally. The wide postorbital process extends caudodorsally behind the orbit and forms the rostral margin of the infratemporal fenestra. It is widely separated from the squamosal, unlike other basal neoceratopsians where the postorbital process contacts the squamosal (e.g., *Liaoceratops, Archaeoceratops*; You and Dodson, 2004). The articular surface for the postorbital is concave and faces rostrolaterally. The postorbital process is mediolaterally thin at its distal aspect, and the medial surface is smooth and flat.

In dorsal or ventral view, the elongate quadratojugal process bows laterally at its mid-length, as in *Chaoyangsaurus* (Zhao et al., 1999) and *Psittacosaurus*, but unlike other basal ceratopsians, which have straight, reduced quadratojugal processes (e.g., *Liaoceratops*). It also expands mediolaterally near its mid-length, forming a prominent lateral eminence, and is subtriangular in cross-section. In *Chaoyangsaurus* and *Psittacosaurus lujiatunensis*, the quadratojugal process also expands transversely, but only at its ventral edge. The narrow dorsal edge forms most of the ventral margin of the infratemporal fenestra.

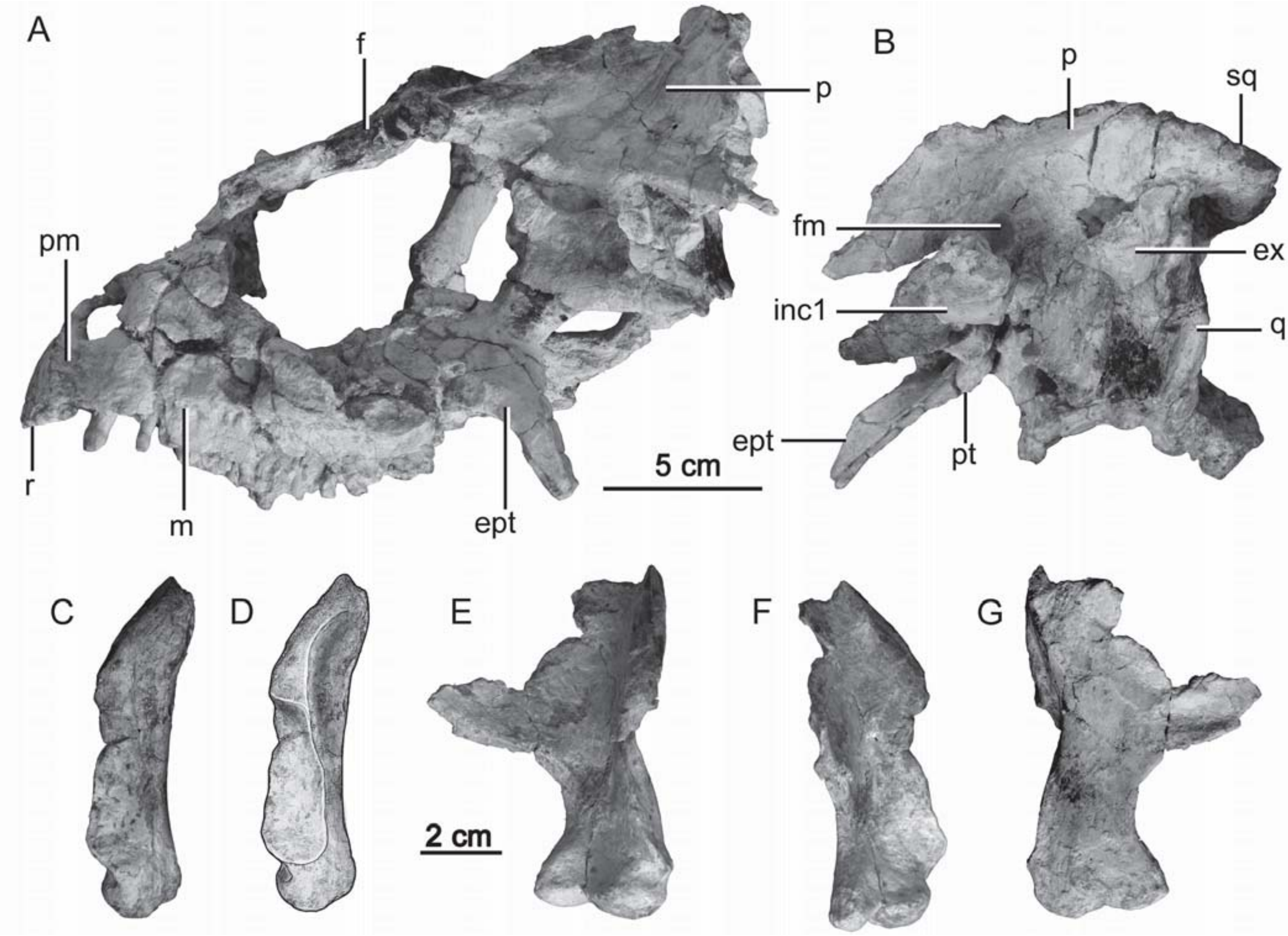

FIGURE 17. *Yinlong downsi* IVPP V18637. **A**, skull in left lateral views; **B**, skull in caudal view; left quadrate in **C**, lateral (photograph), **D**, lateral (drawing), **E**, rostrolateral, **F**, rostral, **G**, caudomedial views. **Abbreviations**: **ept**, ectopterygoid; **ex**, exoccipital; **f**, frontal; **fm**, foramen magnum; **inc1**, atlas intercentrum; **m**, maxilla; **p**, parietals; **pm**, premaxilla; **pt**, pterygoid; **q**, quadrate; **r**, rostral; **sq**, squamosal.

The articulation with the quadratojugal is complex. Distally, the quadratojugal process divides into a small dorsal ramus and a long caudal ramus that tapers caudoventrally to a blunt point. The dorsal ramus is a short rounded process that overlaps a laterally facing facet on the quadratojugal (Fig. 2; the dorsal ramus is incomplete, but the facet on the quadratojugal is clearly defined). The more substantial caudal ramus has a long caudoventrally directed suture with the quadratojugal that terminates on the underside of the quadratojugal near the quadrate, as in *Chaoyangsaurus, Xuanhuaceratops* (Zhao et al., 2006), and *Psittacosaurus* (e.g., *P. lujiatunensis*; IVPP V12617). A sharp ridge is present on the caudal ramus where it contacts the quadratojugal (Fig. 15D), as in *Archaeoceratops* and *Auroraceratops* (Fig. 3; Morschhauser, 2012). However, the suture is more dorsoventrally directed in the latter. In medial view, a rostrocaudal groove extends along the quadratojugal process of the jugal for articulation with the quadratojugal (Fig. 14B).

In overall morphology, the jugal of *Yinlong* is similar to the basal ceratopsians *Chaoyangsaurus* and *Psittacosaurus*, but differs from other neoceratopsians in having a dorsoventrally slender and symmetrical quadratojugal process and a relatively narrow postorbital process that can be seen only partially in lateral view, and lack of contact between the jugal and squamosal.

Quadratojugal—The large quadratojugal is subtriangular and plate-like and covers the entire distal quadrate down to the condyles (Figs. 2–9, 11, 15). The lateral surface is unornamented and lacks a quadratojugal foramen, although a fossa is present on its caudodorsal aspect.

The quadratojugal forms a long, oblique, and complex suture with the quadratojugal process of the jugal, as described above. A deep groove is present along the thickened rostroventral margin of the quadratojugal for most of this contact (Fig. 15F). This groove is present but weakly developed in *Chaoyangsaurus*. The quadratojugal extends caudodorsally to form the caudoventral margin of the infratemporal fenestra between the jugal and quadrate. Although the dorsal end is missing in all specimens, its articular surface on the quadrate indicates that it extended approximately two-thirds of the distance up its rostral margin. It does not appear to have contacted the squamosal, although this cannot be confirmed.

The quadratojugal is fully exposed in lateral view. This is similar to the situation in *Chaoyangsaurus* (Zhao et al., 1999), *Xuanhuaceratops* (Zhao et al., 2006), and *Psittacosaurus* (Sereno, 2010), but unlike neoceratopsians, such as *Liaoceratops, Archaeoceratops*, and ceratopsids, where most of the quadratojugal is concealed by the jugal laterally.

Quadrate—The quadrate consists of the shaft and a rostromedially directed pterygoid wing (Figs. 2, 3, 6, 8, 9, 13,

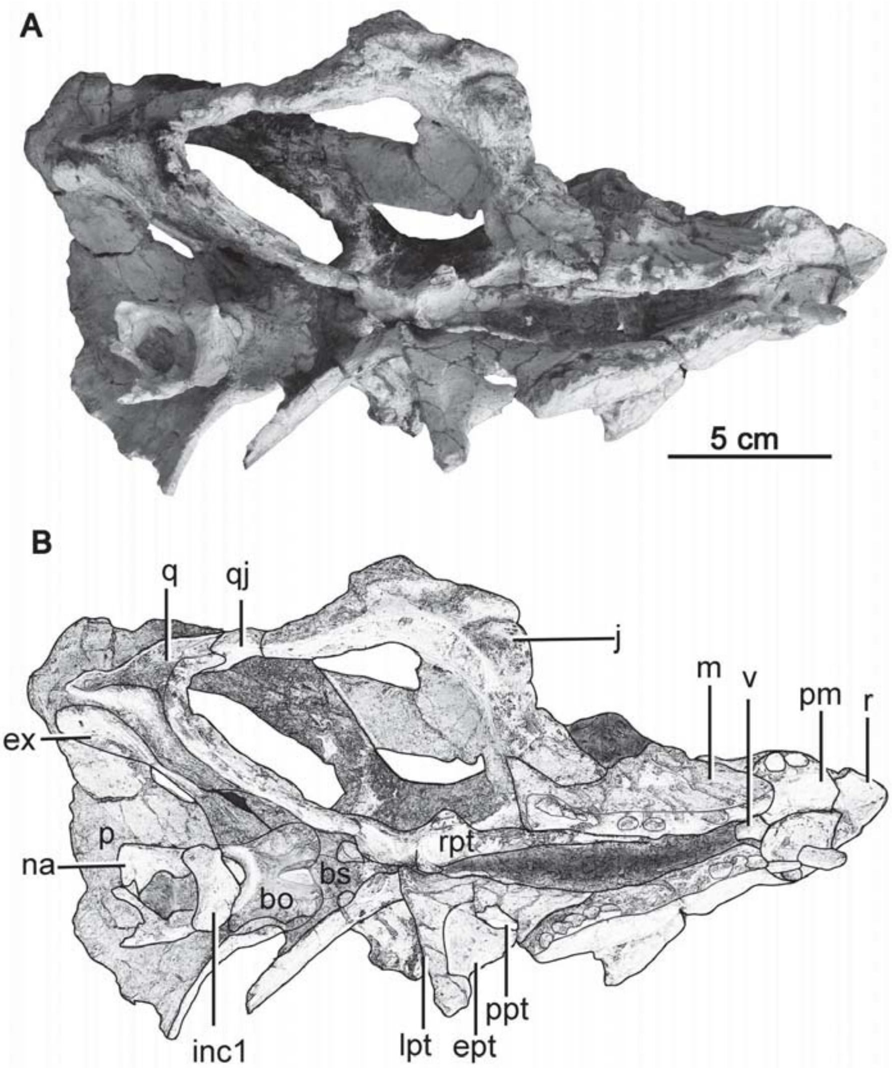

FIGURE 18. *Yinlong downsi* IVPP V18637 skull in ventral view. **A**, photograph; **B**, drawing. **Abbreviations**: **bo**, basioccipital; **bs**, basisphenoid; **j**, jugal; **ept**, ectopterygoid; **ex**, exoccipital; **inc1**, atlas intercentrum; **lpt**, left pterygoid; **m**, maxilla; **na**, neural arch; **p**, parietals; **pm**, premaxilla; **ppt**, pterygoid-palatine fenestra; **q**, quadrate; **qj**, quadratojugal; **r**, rostral; **rpt**, right pterygoid; **v**, vomer.

16–17). The small, rounded quadrate head is triangular in dorsal view, with the apex of the triangle oriented medially. The head fits into a deep cotylus in the underside of the squamosal. A moderately well developed squamosal buttress is present on the proximocaudal margin of the quadrate shaft below the articular head. The exposed surface of the quadrate shaft faces caudolaterally; its rostral margin forms a thick, rugose ridge, as in other basal ceratopsians. The shaft is bowed rostrally, as in other neoceratopsians. The shaft increases in rostrocaudal width distally and reaches its greatest width along the distal quadratojugal facet.

The large quadratojugal facet is slightly concave and is bounded caudally by a well-defined ridge. The facet is widest ventrally but narrows dorsally to a small sulcus at approximately three-fifths of the distance up the quadrate shaft. The rostral margin of the dorsal portion of the quadratojugal facet is incised by a large, obtuse notch that is covered by the quadratojugal when articulated (Fig. 17C, D). This is similar to that of *Liaoceratops*. In caudal view, a small fenestra is present at the midlength of the quadrate shaft, adjacent to the caudodorsal margin of the quadratojugal facet (IVPP V18637), as in other basal neoceratopsians (e.g., *Liaoceratops* [Xu et al., 2002], *Auroraceratops* [Morschhauser, 2012], as well as in *Heterodontosaurus* [Norman et al., 2011]).

The pterygoid wing of the quadrate is a broad sheet of bone that extends rostromedially perpendicular to the caudolateral face of the proximal quadrate. It is broadest at its ventral limit and narrows proximally to meet the shaft near the dorsal-most extent of the quadratojugal facet. It is well separated from the distal quadrate condyles. The pterygoid wing of the quadrate bears a shallow fossa on its medial surface where it overlaps the lateral surface of the quadrate wing of the pterygoid.

The distal quadrate shaft expands into two very broad, rounded condyles that are separated by a deep sulcus. The combined width of the condyles is 30% the length of the quadrate. The lateral condyle is larger and more prominent than the medial one, as in other basal ceratopsians such as *Chaoyangsaurus* (Zhao et al., 1999), *Xuanhuaceratops* (Zhao et al., 2006), *Liaoceratops*, and *Archaeoceratops* (IVPP V11114). They also differ from *Psittacosaurus*, which has flattened condyles (e.g., *P. lujiatunensis*).

Squamosal—The large squamosal forms the caudolateral margins of the skull and the caudal one-third of the lateral margin of the supratemporal fenestra. It has postorbital, parietal, and quadrate processes (Figs. 2–6, 8–13, 16).

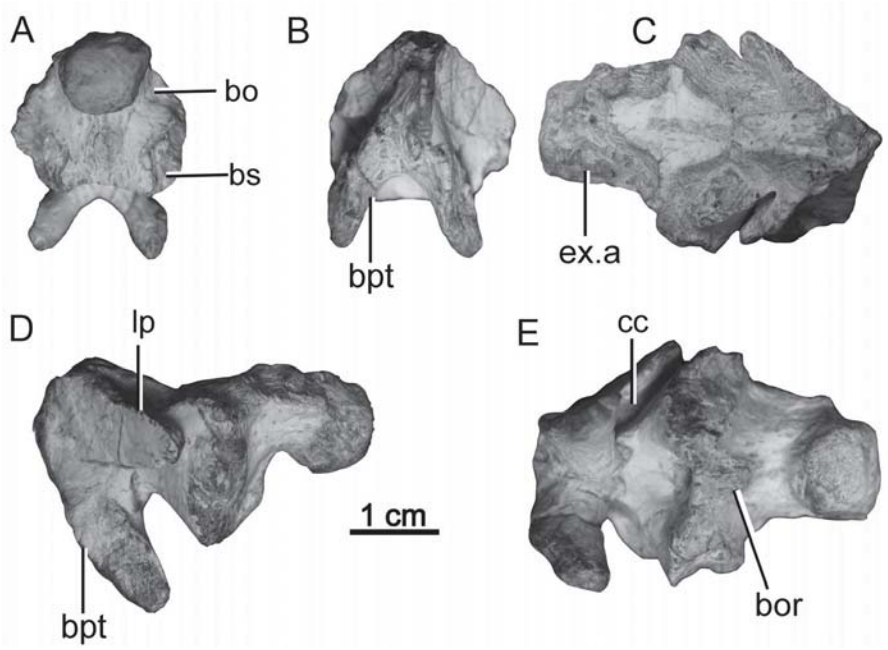

FIGURE 19. *Yinlong downsi* IVPP V14530 fused basioccipital and basisphenoid in **A**, caudal, **B**, rostral, **C**, dorsal, **D**, left lateral, **E**, ventral views. **Abbreviations**: **bo**, basioccipital; **bor**, midline ridge on basioccipital; **bpt**: basipterygoid process; **bs**, basisphenoid; **cc**, carotid canal; **ex.a**, articular surface for exoccipital; **lp**, lateral process on basisphenoid.

The squamosal is expanded dorsally along the skull roof, but contracts strongly ventrally to the stalk-like quadrate process. The squamosal overhangs the quadrate process laterally, and the occiput caudally, and extends further caudally than the parietals. Three to four strongly expanded nodes lie along the caudal and lateral margins of the squamosal, as in pachycephalosaurs (Maryańska et al., 2004). In IVPP V14530, three marginal nodes are present, with the rostral-most node located across the postorbital-squamosal suture. Large and small nodules are also present on the dorsal surface, and all have a rugose, textured surface. In *Liaoceratops*, weak marginal nodes are also present along the caudal margin of the squamosal (Xu et al., 2002:fig. 1) as in most ceratopsians. There is no indication that these nodes are separate ossifications.

The narrow and long quadrate process has a subtriangular cross-section and a strongly concave lateral surface. Its rostral margin forms the caudodorsal portion of the infratemporal fenestra. Distally, the quadrate process divides into a rostral ramus and a slightly shorter caudal ramus. The rostral ramus is subtriangular in cross-section at the base and becomes rostrocaudally compressed ventrally. The caudal ramus is convex caudally and slightly curved ventrally, subtriangular in cross-section, and mediolaterally compressed. These rami flank a deep cotylus that receives the quadrate head.

The quadrate process grades medially into the parietal process, which is rostrocaudally compressed, and dorsoventrally deep. The parietal process extends rostromedially to contact the rostrolateral margin of the parietal, forming a deep, extensive scarf joint, as in other marginocephalians (Sereno, 2000). In caudal view, there is a semilunar fossa across the caudal ramus of the quadrate process and the ventral aspect of the parietal process of the squamosal (Fig. 6) for articulation with the rostrodorsal margin of the paroccipital process. The postorbital process tapers rostromedially to form a long, straight, obliquely oriented suture with the postorbital. It is subtriangular in cross-section, and its entire ventrolateral surface overlaps the postorbital.

In overall morphology, the squamosal differs from all other known basal ceratopsians in its stalk-like quadrate process and large nodes on both the dorsal surface and margin. Unfortunately, no squamosal is present in the basal ceratopsians *Chaoyangsaurus* and *Xuanhuaceratops* for comparison.

Parietal—The parietals roof the braincase and contribute substantially to the medial and caudomedial margins of the supratemporal fenestrae (Figs. 3–6, 8–10, 16–18). The parietals form a strong, sharp sagittal crest where the left and right supratemporal fossae meet, as in other basal ceratopsians such as *Liaoceratops* (Xu et al., 2002) and *Archaeoceratops* (You and Dodson, 2003), *Psittacosaurus* (Sereno, 2010), and *Heterodontosaurus* (Norman et al., 2011). The parietals are narrow along the braincase and slope strongly ventrally along the inner margins of the supratemporal fenestrae. Rostrally, the parietals expand laterally to form broad peg-in-socket joints with the rear of the frontals, but do not contact the postorbitals.

A moderately deep notch is present on the midline of the parietals at their caudal margin, as in some *Psittacosaurus* (e.g., *P. lujiatunensis*: ZMNH M8138; *P. mongoliensis*) and small specimens of *Liaoceratops*, but unlike large *Liaoceratops* individuals where the entire caudal margin is convex (Xu et al., 2002). Although the caudal margin of the parietals extends slightly over the occiput, particularly near its midline, it does not extend as far as that of the squamosal. In dorsal view, the caudal margin of the parietosquamosal frill is sinuous, with deep incursions between the parietals and squamosals (Fig. 10). In *Psittacosaurus*, the squamosal and parietals extend caudally to the same level, and the parietals exceed the squamosal in length in most neoceratopsians (e.g., *Liaoceratops, Protoceratops*).

The squamosal processes of the parietals are deep and rostrocaudally compressed; they have extensive vertical sutures with the parietal processes of the squamosals. In dorsal view, they are slightly 'S'-shaped in IVPP V18684 and IVPP V18636 and relatively straight in the large specimens IVPP V14530 and IVPP V18637. The ventral surface of the parietal shelf bears a low, sharp midline ridge that may have extended ventrally to meet the supraoccipital. The contacts between the parietals, supraoccipital, and braincase are not well preserved in any specimens.

Supraoccipital—The supraoccipital is partially preserved in IVPP V18636 and IVPP V18637, but the margins of the element are not preserved (Fig. 9). The supraoccipital contributes to the dorsal

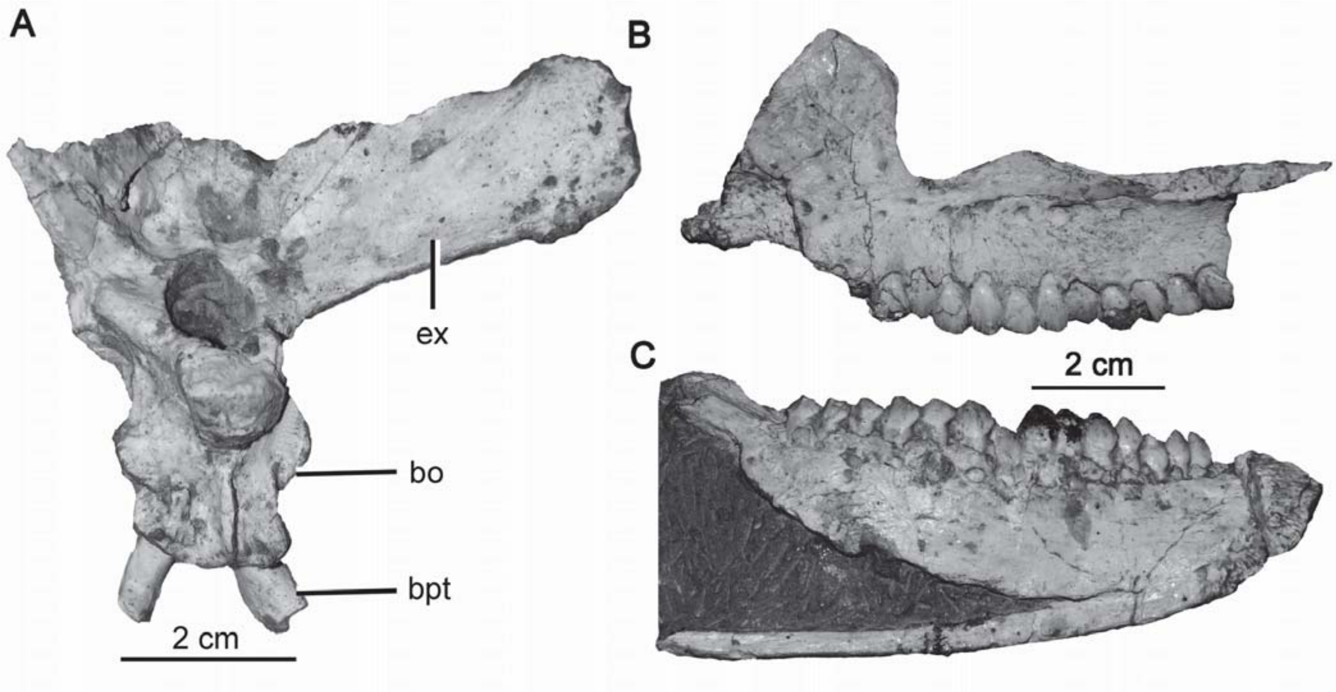

FIGURE 20. *Yinlong downsi* IVPP V18684. **A**, occiput in caudal view; **B**, left maxilla in lateral view; **C**, left dentary medial view. **Abbreviations**: **bpt**, basipterygoid process; **bo**, basioccipital; **ex**, exoccipital.

margin of the foramen magnum and bears a midline ridge that was likely continuous with that on the underside of the parietal shelf.

Exoccipital—The exoccipital is only partly preserved in all specimens where it is present (Figs. 6, 9, 17B, 18). The pedicle of the exoccipital overlaps the dorsal surface of the basioccipital to form a small portion of the dorsolateral occipital condyle, and the lateral and ventrolateral margins of the foramen magnum. The exoccipitals do not contact one another around the foramen magnum, being separated by the intervening supraoccipital dorsally and the basioccipital ventrally.

The exoccipital extends caudolaterally to form the paroccipital process. It is dorsoventrally narrow and rostrocaudally thick at the base and becomes progressively deeper and thinner distally, as in other ceratopsians (e.g., *Liaoceratops*). The paroccipital process is subrectangular and asymmetrical, as in other neoceratopsians. The paroccipital process overlaps the caudoventral margin of the squamosal and the caudal margin of the proximal quadrate. The caudal surface of the paroccipital process is smooth and flattened, but the rostral surface is striated (Fig. 6). A prominent caudolaterally facing foramen is present at the mid-length, adjacent to the dorsal margin, in rostral view. A relatively smaller foramen occurs in the same position in *Liaoceratops*.

Basioccipital—The basioccipital extends caudally and slightly ventrally to form most of the convex and spheroidal occipital condyle (Figs. 19, 20). The transverse diameter of the foramen magnum is approximately equal to the width of the condyle, as in *Chaoyangsaurus* (Zhao et al., 1999), but unlike *Liaoceratops* and *Archaeoceratops*, which have a relatively larger foramen magnum. The condylar neck is constricted in lateral view, but flares rostrally in dorsal view. The dorsal surface of the basioccipital is concave on the midline where it floors the rear of the braincase, which deepens into a distinct sulcus caudally. The rugose articular facets for the exoccipitals face dorsolaterally.

The basioccipital flares strongly laterally and ventrally, to approximately twice the depth and width of the occipital condyle, to contact the basisphenoid. The basioccipital has a tight and extensive contact with the basisphenoid and together they form the basal tubera, which are gently ‘W’-shaped in outline in ventral view. The rostral surface of the basioccipital bows rostrally and inserts into the concave caudal margin on the basisphenoid (Fig. 19B). The basal tubera form a thin plate along the midline but are much thicker and more robust laterally, unlike the lateroventrally expanded, thin, and plate-like basal tubera in pachycephalosaurids (Maryańska et al., 2004; contra Xu et al., 2006). A robust midsagittal crest is present on the ventral surface of the basioccipital immediately behind the basal tubera, extending as far as the condylar neck, as in pachycephalosaurids (Sullivan, 2006; Fig. 6D), some basal ornithopods such as *Jeholosaurus* (Barrett and Han, 2009) and *Changchunsaurus* (Jin et al., 2010), and some basal ceratopsians such as *Liaoceratops* (IVPP V12617), *Archaeoceratops* (IVPP V11114; weakly developed), and *Auroraceratops* (Morschhauser, 2012). The basioccipital does not overlap the ventrolateral region of the basisphenoid, so that the basisphenoid is seen in caudal view, as in pachycephalosaurids (Maryańska et al., 2004).

Basisphenoid—The basisphenoid has paired basipterygoid and lateral processes (Figs. 18–20). Its dorsal surface forms a narrow portion of the floor of the braincase. The element is mediolaterally narrow rostrally, but widens substantially to meet the basioccipital caudally. The caudal margin of the robust basisphenoid is concave and ‘U’-shaped in dorsal view to envelop the rostral surface of the basioccipital. The ventral surface of the basisphenoid immediately rostral to the basal tubera has a shallow fossa, as in other ceratopsians such as *Yamaceratops, Protoceratops*, and *Bagaceratops* (Makovicky and Norell, 2006), and some ornithopods, such as *Jeholosaurus* (IVPP V12529).

The lateral processes extend caudolaterally from the body of the basisphenoid immediately in front of the basal tubera. These tapered processes are rostrocaudally compressed and bound the rostral margin of the carotid canal (the tubera form the caudal

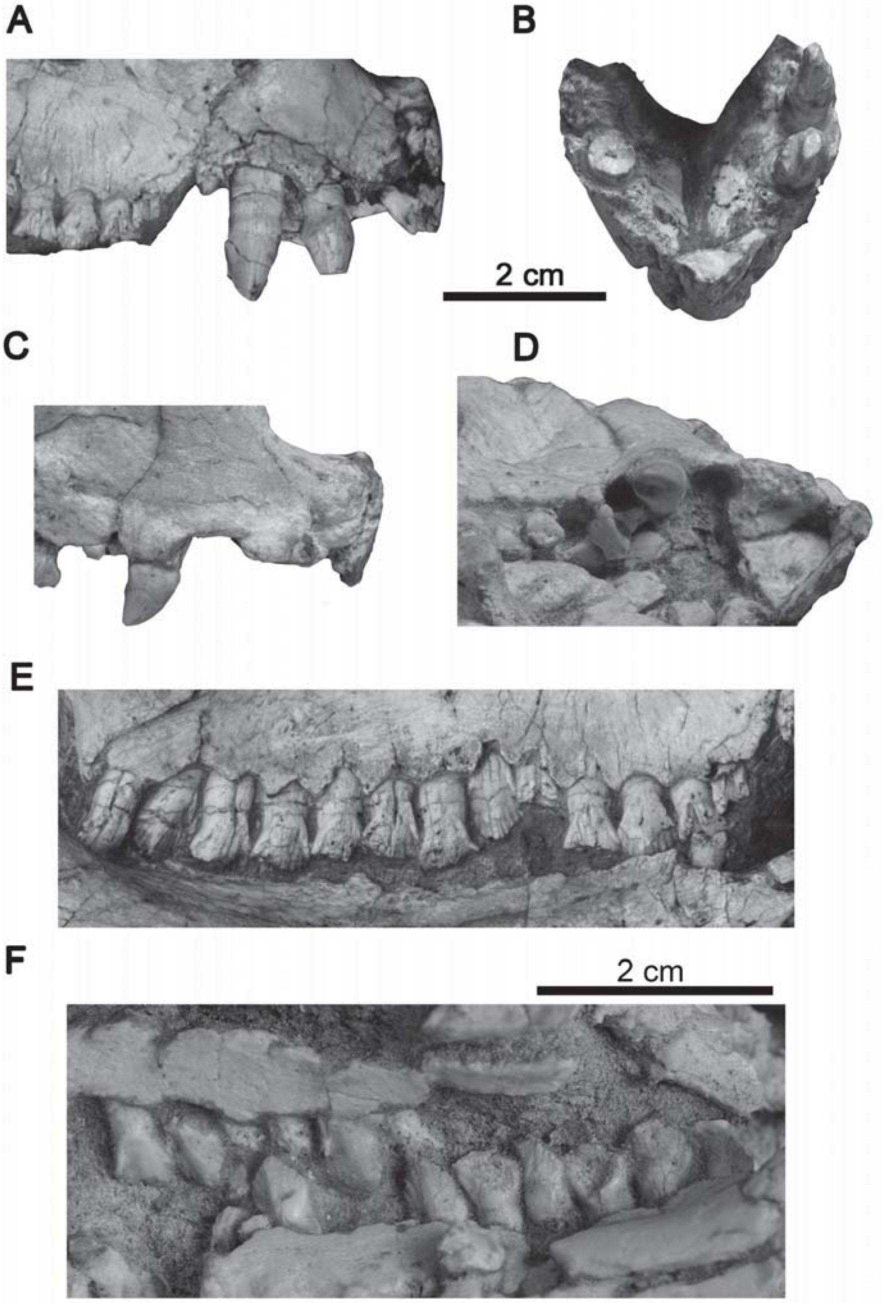

FIGURE 21. Teeth of *Yinlong downsi*. **A**, **B**, **E**, IVPP V14530: **A**, premaxillary and rostral maxillary teeth in lateral view; **B**, premaxillary teeth in ventral view; **E**, right maxillary teeth in lateral view; **C**, **D**, **F**, IVPP V18636: premaxillary teeth in **C**, right lateral, **D**, ventral views; **F**, right maxillary and dentary teeth in lateral view.

margins of the canal). The basipterygoid processes arise below the lateral processes and extend caudoventrally, as in some leptoceratopsids (Chinnery and Weishampel, 1998; Makovicky, 2001), but unlike other ceratopsians where they are ventrally or rostroventrally directed (Dodson et al., 2010). They extend well below the basal tubera and are subtriangular in cross-section. The elliptical, rostrolaterally facing articular facet for the pterygoid is well developed on its distal aspect. The processes diverge from each other at an angle of approximately 60° (IVPP V14530). The dorsolateral margin of the basisphenoid is rugose for contact with the prootic.

Pterygoid—The pterygoids contact on the midline at the point where the three plate-like rami (palatine, maxillary, quadrate) converge (Figs. 6, 16–18). Together the pterygoid, ectopterygoid, and palatine form a large oval pterygopalatine fenestra adjacent to the rear end of the maxillary tooth row, as in other basal ceratopsians such as *Liaoceratops* (Xu et al., 2002), *Chaoyangsaurus* (Zhao et al., 1999), *Psittacosaurus* (Zhou et al., 2006), and *Yamaceratops*. This fenestra is reduced in more derived ceratopsians (Makovicky and Norell, 2006).

The palatine ramus is subtriangular and extends rostrodorsally (Fig. 17; contra Xu et al., 2006). This is similar to the condition in *Chaoyangsaurus* (IGCAGS V371), but is not as steeply inclined as in other basal neoceratopsians such as *Liaoceratops* (IVPP V12738). The rostral end is not preserved in any specimen, and its contact with the vomer and palatine are not clear.

The ectopterygoid ramus extends laterally as a slender sheet of bone that has an extensive contact with the caudomedial surface of the ectopterygoid. In caudal view, the ramus is slightly curved ventrally, unlike other basal neoceratopsians, such as *Chaoyangsaurus* (IGCAGS V371) and *Liaoceratops* (IVPP V12738), in which it is strongly curved ventrally. In rostroventral view, the rostral margin of the ectopterygoid ramus is concave and arched from its base to nearly 75% of its entire length. This feature is also seen in *Liaoceratops* (IVPP V12738) and *Chaoyangsaurus* (IGCAGS V371), but seems to be absent in *Auroraceratops* (Morschhauser, 2012) and *Yamaceratops* (Makovicky and Norell, 2006).

The quadrate ramus flares caudolaterally and broadly overlaps the fossa on the medial surface of the pterygoid process of the quadrate. A small caudally directed process arises medially from the thickened base of the quadrate process for articulation with the pterygoid processes of the basisphenoid (Figs. 6, 18, 20), bracing the palate against the braincase. This process is short in *Yinlong*, unlike most basal neoceratopsians such as *Liaoceratops* (Xu et al., 2002) and *Auroraceratops* (You et al., 2005), which have elongate processes that cover the basipterygoid processes.

Ectopterygoid—The ectopterygoid is a complex bone that forms the caudal margin of the pterygopalatine foramen (Figs. 6, 16–18). It is relatively large and separates the pterygoid from the maxilla, as in basal ceratopsians, such as *Liaoceratops* (IVPP V14530), but unlike in other neoceratopsids and ceratopsids, which have much reduced ectopterygoids that are concealed in ventral view (Dodson et al., 2004).

The ectopterygoid tapers ventrolaterally and curves medially to overlap the dorsolateral surface of the pterygoid. A well-developed ridge extends along the rostrolateral edge of the ectopterygoid, giving it a triangular cross-section. This ridge is sharp at its mid-length, but blunt toward each end (Fig. 17A, B). The ectopterygoid extends laterally to contact the caudomedial surface of the rear of the maxilla and medial surface of the maxillary process of the jugal. The well-defined maxillary facet is smooth and concave, whereas the jugal facet is rugose and expands in all directions.

Palatine—A partial palatine is preserved in IVPP V18637 (Fig. 18). It is plate-like, mediolaterally compressed, and dorsoventrally expanded. In ventral view, the palatine is wedge-shaped rostrally, deepens caudally, and overlaps the medial surface of the caudal maxilla. It forms the rostral margin of the pterygopalatine foramen and contacts the pterygoid medially and dorsally.

Vomer—The rostral regions of the fused, rod-like vomers are preserved in IVPP V18637 (Fig. 18). In ventral view, the rostral ends expand into a diamond shape that inserts into the rear margin of the paired premaxillae and appear to separate the maxillae on the midline, although this cannot be confirmed.

Prootic, Laterosphenoid—These elements are either missing or not exposed in all known specimens.

Mandible

The mandibles are articulated with the skull in IVPP V14530, IVPP V18636, and IVPP V18686, but separate and partially preserved in IVPP V18640 and IVPP V18684 (Figs. 2–4, 7–11, 15, 20).

Predentary—The predentary covers the rostroventral end of the dentary symphysis and supports two short dorsolateral processes and one ventral process (Figs. 2–3, 5, 7–8, 10, 11). The predentary is much shorter than the premaxilla, and when the skull and mandible are articulated, the rostral end of the predentary does not reach the rostral bone, as in *Chaoyangsaurus* and some *Psittacosaurus*, but unlike that of neoceratopsians (e.g., *Liaoceratops, Archaeoceratops*; Sereno, 1990; Zhao et al., 1999; You and Dodson, 2004).

The predentary is triangular in dorsal and lateral views. The inner surface is concave. A rounded midline keel is developed in IVPP V14530, but is not sharply defined. However, the outer surface of the predentary is gently rounded and unkeeled in IVPP V18636, as in *Psittacosaurus* and the basal neoceratopsians *Liaoceratops* and *Archaeoceratops*. Several small nutrient foramina are present on the lateral surface of the predentary below the oral margin. In lateral view, the oral margin appears nearly horizontal. The narrow triturating surface is nearly flat rostrally, but becomes slightly convex caudally.

The broad, long ventral process of the predentary extends caudoventrally to overlap the ventral surface of nearly the entire dentary symphysis. Xu et al. (2006) considered that the caudal margin is bifurcated. However, the distal edge is damaged in all specimens; thus, this cannot be confirmed. This process is gently rounded across its rostral margin. The paired lateral processes are relatively short and blunt and narrower than the ventral process. The lateral process fits into a facet on the dorsolateral margin of the rostral part of the dentary, and when the skull and mandible are articulated, it terminates at approximately the premaxilla-maxilla suture at the oral margin. The dorsal and ventral processes meet at a well-defined, acute angle. The lateral surface of the predentary is smoothly rounded and lacks a longitudinal groove separating the lateral and ventral processes, which occurs in ornithopods, such as *Jeholosaurus* (Barrett and Han, 2009).

Dentary—The articulated dentaries diverge caudally, and each contains 15 teeth (IVPP V18684; Figs. 2, 3, 7–11, 15, 20). The rostral regions of the paired dentaries are angled medially to form a long symphysis. The symphyseal surfaces are flat. The dentary is shallow, with a dorsoventrally convex lateral surface rostrally, but becomes progressively deeper and wider, and the surface flatter, caudally. There is no defined cheek emargination. In lateral view, the oral margin is slightly bowed downward; in dorsal view, the tooth row is bowed slightly medially.

The dentary has two articular surfaces for the predentary: a narrow concave facet for the dorsal process and a broad flat articulation for the ventral process. A large neurovascular foramen exits the dentary where the dorsal and ventral processes of the predentary diverge. Additionally, six axially elongate neurovascular foramina are present below the oral margin on the lateral surface, beginning below the first dentary tooth. Caudally, they increase in size, more closely approach the oral margin, and are separated by progressively larger distances between adjacent foramina. Several smaller foramina are also present on the lateral surface adjacent to the ventral margin of the dentary. Medially, the surface of the dentary is flattened to contact the splenial. Meckel's groove narrows rostrally and appears to extend to the dentary symphysis.

The dentary tooth row terminates rostral to the coronoid process without an intervening sulcus, as in *Chaoyangsaurus* (Zhao et al., 1999), but unlike *Psittacosaurus* (Sereno, 1990) and neoceratopsians such as *Archaeoceratops* (You and Dodson, 2003) and *Yamaceratops* (Makovicky and Norell, 2006). Behind the tooth row, the dentary extends caudodorsally to form the rostral portion of the coronoid process and the highest point of the mandible. The coronoid process reaches well above the level of the tooth row. The caudal margin of the dentary overlaps the rostral margin of the angular and surangular; the small subcircular external mandible fenestra is formed at the junction of these three elements.

Surangular—The large surangular is long, shallow, and subrectangular in lateral view (Figs. 2–3, 5–8, 15). It is slightly shorter rostrocaudally than the dentary, as in *Chaoyangsaurus* (Zhao et al., 1999) and *Psittacosaurus* (Sereno, 2010), whereas the surangular is much shorter than the dentary in neoceratopsians such as *Liaoceratops* and *Archaeoceratops* (Xu et al., 2002; You and Dodson, 2003).

The surangular forms the caudodorsal portion of the caudally sloping coronoid process, and the upper half of the caudal region of the mandible. It is overlapped by the dentary along its convex rostral margin. In lateral view, the dorsal margin of the surangular is gently convex, whereas the ventral margin is gently concave where it meets the angular. The angular broadly overlaps the lateral and ventral surfaces and stopped bellow the glenoid fossa. The rostroventral corner of the surangular contributes to the external mandibular foramen. A small foramen pierces the surangular near its rostral margin, centered dorsoventrally. A similar fenestra is also present in other ornithischians, such as *Jeholosaurus* and *Scelidosaurus* (NHMUK R1111).

Rostral to the glenoid fossa, the surangular is a fairly thin plate that forms the lateral wall of the internal mandibular fenestra. Approaching the glenoid, the surangular abruptly broadens medially, then flares laterally, to form the lateral portion of the glenoid fossa and the lateral half of the retroarticular process. Here it is strongly convex laterally. It forms the lateral cotylus of the glenoid fossa, and a ventromedially facing articular surface for the articular. The glenoid fossa occurs at the level of the tooth row. The surangular cotylus is deep and nearly twice as wide as its rostrocaudal length. The surangular forms the lateral portion of the robust but short retroarticular process, as in other basal neoceratopsians such as *Liaoceratops* and *Chaoyangsaurus* (Zhao et al., 1999), but different from *Psittacosaurus*, which has a long retroarticular process (Sereno, 1990).

A small surangular foramen is present rostroventral to the surangular glenoid on the lateral surface. A prominent rostroventrally oriented tubercle is present rostroventral to the surangular foramen, adjacent to the junction with the angular (Fig. 2). This tubercle extends laterally to overhang the angular. Immediately in front of the glenoid fossa on the medial surface is a sharp, dorsoventrally compressed, shelf-like process whose base defines the rear of the internal mandibular fenestra. The caudoventral surface of this process articulates with the front of the articular, and its rugose medial surface articulates with the dorsal margin of the prearticular (Fig. 15I).

Articular—The articular is subrectangular in dorsal view, expanding gently caudally to form the slightly concave medial glenoid cotylus (Fig. 6). Its lateral surface is covered by the surangular, and its ventral and medial surfaces are tightly wrapped by the prearticular. In caudal view, a deep depression is present on the caudal surface of the right articular. The articular is expanded medially and is semilunate in caudomedial view, a feature uniquely shared with chaoyangsaurids (Zhao et al., 2006).

Angular—The angular is a strap-like element approximately 80% the length of the surangular and comprises approximately the lower half of the caudal portion of the mandible (Figs. 2–3, 5, 7, 8, 10–11, 15). The angular is deep rostrally but tapers caudodorsally to the glenoid fossa. The inclined ventral margin of the angular forms an angle of 30° with the dentary tooth row, similar to the basal ceratopsian *Chaoyangsaurus* (Zhao et al., 1999).

A prominent lateral ridge is present on the caudoventral angular subparallel to its ventral margin. This ridge terminates adjacent to the tubercle on the surangular. The surface of the angular above this ridge is depressed and smooth, but is heavily textured below it. This feature also occurs in *Xuanhuaceratops* (IVPP V12722) and *Chaoyangsaurus* (Zhao et al., 2006).

The rostrodorsal margin of the angular forms the caudoventral margin of the external mandibular fenestra. Below this, the rostral angular is overlapped by the dentary laterally and ventrolaterally, and by the splenial ventromedially, as in *Chaoyangsaurus* and *Psittacosaurus*, but unlike all other neoceratopsians in which a rostral process extends from the ventral edge of the angular to overlap the dentary (Makovicky and Norell, 2006).

The angular wraps medially to form the ventral margin of the rear of the mandible. The ventral surface of the angular is convex transversely in the rostral region and flattened towards the caudal end.

Splenial—The splenial is subtriangular in outline, concave medially, and overlaps most of the medial surface of the dentary (IVPP V14530; Fig. 7). It is a substantial element in *Yinlong* and accounts for nearly half the width of the mandible where present. Rostrally, the splenial tapers to a point along the ventral edge of the dentary and appears to have reached to the dentary symphysis, although this cannot be confirmed in any specimen.

Caudally, the splenial expands dorsoventrally to cover the internal surface of the dentary and forms the curved rostral margin of the internal mandibular fenestra. Caudal to this point, the splenial continues along the ventral margin of the internal mandibular fenestra as a tapering process that abuts the ventral dentary, overlaps a facet along the ventromedial margin of the angular, and overlaps the rostral margin of the prearticular. It terminates in a blunt tip near the midpoint of the angular.

Prearticular—The prearticular is a slender, rod-like element (IVPP V14530; Fig. 7). A longitudinal facet is present along the ventral surface of the prearticular to articulate with the surangular. The prearticular expands dorsoventrally and twists slightly medially at the caudal end of the mandible. It covers the ventral and medial surfaces of the articular and is overlapped by the splenial rostrally.

Dentition

The dentition has been described in Tanoue et al. (2009). However, the specimens described here provide additional information, and a full description is presented.

Premaxillary Teeth—Three premaxillary teeth are present (Figs. 2, 8, 11, 17A, 21). The first tooth is well separated from the rostral margin of the premaxilla by an edentulous region. The second tooth is slightly larger than the first, and both exceed all maxillary teeth in size, as in some heterodontosaurids, such as *Heterodontosaurus* and *Tianyulong* (Zheng et al., 2009; Norman et al., 2011). The third tooth is much smaller than the first two, whereas the third tooth is the largest in heterodontosaurids. The third premaxillary tooth is positioned adjacent to the junction between the premaxilla and maxilla. The teeth are enameled on all surfaces.

The premaxillary tooth crowns are semiconical and do not curve at the tip. However, in IVPP V18636, the tip of the left second premaxillary tooth curves slightly caudally, and the blade-like crown has a straight distal carina and a strongly curved mesial carina (Fig. 21C). This caniniform morphology is similar to that of theropod teeth and also occurs in some heterodontosaurids (Sereno, 2012) and pachycephalosaurs (Maryańska et al., 2004). This may represent individual variation or possibly sexual dimorphism (Thulborn, 1974).

The crowns are slightly labiolingually compressed, with the lingual surface flattened and the labial rounded. The flattened lingual surface tends to be aligned with the curve of the premaxilla; for example, the flat surface of the second tooth, at the widest part of premaxilla, is oriented in the sagittal plane, whereas the surface of the first tooth is oriented mesiolingually, nearly in line with the oral margin of the premaxilla. The lingual surface differs between the first and second teeth. In the first tooth, there is an abrupt step between the inflated base and more distal, lingually flattened crown. This is unique to *Yinlong* (Xu et al., 2006). This step is present but more weakly developed in the second and third premaxillary teeth (Fig. 21B, D). The roots are circular in cross-section.

Several longitudinal ridges extend from the base of each tooth to the tip on the labial side; these are not present on the flattened lingual surface. Both the mesial and distal carinae of the premaxillary teeth bear fine denticles on all teeth (Tanoue et al., 2009). In IVPP V18636, there are seven denticles on the margin of the second premaxillary tooth; the denticles are wide at the base and taper to their tip. The mesial denticles are weak, and their number and morphology are difficult to determine.

Maxillary Teeth—The maxilla bears 13 teeth in all specimens (IVPP V14530, IVPP V18636, IVPP V18638, IVPP V18684; Figs. 12, 20, 21). The first four maxillary teeth are relatively small, and the more distal teeth are larger and subequal to each other in size. In lateral view, the maxillary teeth are slightly bulbous at the base and expand mesiodistally toward the tip of the crown. The crowns of the maxillary teeth are imbricated so that the distal margin of each tooth crown overlaps the mesial margin of the tooth behind it. Most of the crowns lack primary and secondary longitudinal ridges (Fig. 21E), although some distal teeth bear weak to prominent ridges (Fig. 21F). Large, tongue-shaped denticles are present along the mesial and distal carinae of tooth crowns. All the denticles are subequal in size and taper distally. The mesial and distal marginal ridges are prominent and support large basal denticles as in derived neoceratopsians, such as *Protoceratops* (Tanoue, 2009). This feature is present but weak in *Chaoyangsaurus, Psittacosaurus, Liaoceratops*, and *Archaeoceratops* (Tanoue, 2009; Sereno, 2010).

Dentary Teeth—The dentary teeth are similar to the maxillary teeth in morphology (Figs. 20, 21F). The teeth in the middle region of the dentary tooth row are relatively larger than in the mesial and distal regions. The mesial teeth are more elongate and less expanded at the base, and the crown tip is slightly recurved. The crowns are imbricated, with the mesial margin of the each crown overlapping the distal margin of the crown behind it. The tooth crown becomes wider and lower towards the caudal end of the dentary. Most of the tooth crowns lack primary or secondary ridges, although teeth at the rostral or caudal end of the tooth row occasionally bear weak ridges. Five or six large denticles are present on the mesial and distal carinae of the tooth crowns, as in the maxillary teeth.

DISCUSSION

Yinlong downsi represents the earliest and most complete basal ceratopsian and possesses many autapomorphies (Xu et al., 2006). Three additional autapomorphies are recognized here: large oval nodules concentrated on the lateral surface of the jugal, a deep sulcus on the ventral surface of the quadratojugal, and a squamosal with an inset, stalked quadrate process and a strongly expanded dorsal surface. *Chaoyangsaurus* and *Xuanhuaceratops* represent the only other ceratopsians that may occur in the Late Jurassic (Zhao et al., 1999; Zhao et al., 2006). However, these taxa are known from incomplete material, and their age remains controversial (Xu et al., 2012).

Phylogenetic relationships of basal ceratopsians are not yet fully resolved, due in part to conflicting data. The relationships of *Yinlong* have not been considered in detail, and a phylogenetic analysis would be premature. Here we discuss some of the conflicts in shared characters in the context of current ceratopsian taxonomy.

Zhao et al. (2006) proposed the name Chaoyangsauridae to include *Chaoyangsaurus* and *Xuanhuaceratops*. Three synapomorphies were proposed to support this clade: a deep ventral expansion of the medial process of the mandibular glenoid, a short contact between the quadratojugal and quadrate, and rugose sculpturing on the lateral surface of the dentary. However, a short contact between the quadratojugal and quadrate also occurs in *Liaoceratops* (IVPP V12738) and *Archaeoceratops* (IVPP V11114), and rugose sculpturing on the dentary occurs in *Archaeoceratops* (IVPP V11114) and *Auroraceratops* (Morschhauser, 2012). These two characters thus have a broader distribution among basal ceratopsians. A deep ventral expansion of the glenoid remains valid for Chaoyangsauridae; this feature is also present in *Yinlong*. Additionally, *Yinlong* shares another feature with *Chaoyangsaurus* and *Xuanhuaceratops*: a laterally expanded ridge along the ventral edge of the angular. Although this ridge is partially damaged in *Chaoyangsaurus* and *Xuanhuaceratops*, it still can be confirmed from the preserved material. This ridge is not known in other ceratopsians. These two characters may prove to be primitive for Ceratopsia as a whole or, alternatively, place *Yinlong* within the Chaoyangsauridae.

Chaoyangsaurus and *Xuanhuaceratops* have several derived features absent in *Yinlong*. Only two premaxillary teeth are present in *Chaoyangsaurus* and one in *Xuanhuaceratops*; they are absent in *Psittacosaurus* (Sereno, 1987) and derived ceratopsids (Dodson et al., 2004). The rostral end of the dentary is strongly curved dorsally in *Xuanhuaceratops*, as in the derived neoceratopsians *Leptoceratops* (Sternberg, 1951) and *Protoceratops*. Interestingly, *Chaoyangsaurus* and *Psittacosaurus* share a number of characters, including a tall rostral margin of the skull that is perpendicular to the tooth row, a prominent ridge on the maxilla near the suture with the jugal, and the ventral surface of the quadratojugal process of the jugal flattened and expanded transversely.

Yinlong also shares some characters exclusively with *Chaoyangsaurus* and *Psittacosaurus*. The maxillary ramus of the jugal is much shorter than the quadratojugal ramus, whereas it is reversed in pachycephalosaurians, basal neoceratopsians, and the basal ornithischian *Lesothosaurus* (Maryańska and Osmólska, 1974; Sereno, 1991). Additionally, the ventral surface of the jugal is transversely expanded, as in *Chaoyangsaurus* and *Psittacosaurus*. Moreover, the length of the surangular is nearly equal to that of the dentary, as in *Chaoyangsaurus* and *Psittacosaurus*, but unlike neoceratopsians and other ornithischians that have a much shorter surangular.

Yinlong also shares many neoceratopsian features: rugose sculpturing on the jugal and angular, basipterygoid processes extending ventrally or caudoventrally, postorbital and supratemporal bars that are broad and robust, a short retroarticular process, and the presence of a foramen on the mid-portion of the quadrate shaft in caudal view. All these characters are present in the basal neoceratopsians *Liaoceratops* and *Archaeoceratops*, but are absent in *Psittacosaurus* (Sereno, 2010). However, *Yinlong* lacks derived characters of neoceratopsians such as a jugal horn and epijugal; a jugal horn is present in *Psittacosaurus* and all neoceratopsians, and an epijugal is present in derived neoceratopsians except *Liaoceratops* and *Archaeoceratops*. *Yinlong* lacks a caudally expanded parietosquamosal frill as occurs in *Liaoceratops, Auroraceratops* (Morschhauser, 2012), and more derived neoceratopsians (You and Dodson, 2004). The antorbital fossa is very deep and sharply defined rostrally in *Yinlong*. However, the antorbital fossa of *Liaoceratops* is shallow rostrally, with a weakly defined margin. This rostral definition is absent in *Archaeoceatops* and more derived ceratopsians (You and Dodson, 2003). The postorbital and jugal bar is narrower than the infratemporal fenestra in *Yinlong*, unlike other basal neoceratopsians where the former is wider than the latter. Overall, *Yinlong downsi* shares derived characters with both *Psittacosaurus* and neoceratopsians, suggesting that character evolution in basal ceratopsians is complex.

Yinlong downsi shares derived characters with heterodontosaurids and pachycephalosaurs and supports the monophyly of marginocephalians and the close relationship of heterodontosaurids to marginocephalians (Xu et al., 2006). However, all recent ornithischian phylogenetic analyses place heterodontosaurids as the most basal ornithischians (Butler et al., 2008; Norman et al., 2011). Here we also found an additional derived character shared by *Heterodontosaurus* and basal ceratopsians: a sharp parietal midline crest. However, this character is absent in all pachycephalosaurs where known, and no information exists for more basal pachycephalosaurs (Maryańska et al., 2004).

Marginocephalian monophyly has been well supported in many recent phylogenetic analyses (Xu et al., 2006; Butler and Zhao, 2009; Han et al., 2012). However, some synapomorphies of marginocephalians may need to be reconsidered and modified. For example, the morphology of the basal tubera of *Yinlong* was considered to be similar to the condition in pachycephalosaurs (Xu et al., 2006). However, the basal tubera are thin near the midline but robust laterally in *Yinlong*, unlike the flattened and plate-like basal tubera in pachycephalosaurs (Maryańska et al., 2004). The nodular ornamentation on the squamosal and postorbital is shared by basal ceratopsians and pachycephalosaurs and was considered as the same character state in recent ornithischian phylogenies, such as Butler et al. (2008). However, in basal ceratopsians, the surface of the ornamentation is rugose and sculptured, whereas it is smooth in pachycephalosaurs (Evans et al., 2011; Schott and Evans, 2012). These differences require more discussion and comparison, including histological study of the condition in relevant taxa.

The relatively good sample of skulls and mandibles of *Yinlong downsi* shows ontogenetic variation in this taxon. Smaller individuals (IVPP V14530, IVPP V18636) have relatively smaller rostral bones and shorter and wider frontals than larger specimens (e.g., IVPP V18637). Both these characters have been employed in phylogenetic analyses of ornithischians (Xu et al., 2006; Butler et al., 2008) and must be reconsidered in future analyses. Nodules on the squamosal are absent or weak in small individuals (IVPP V18638, IVPP V18636) (Figs. 10, 13) and well developed in larger ones (IVPP V14530, IVPP V18637). Another feature that may relate to ontogenetic variation is that the caudal margin of the parietosquamosal shelf is strongly curved and 'S'-shaped in smaller individuals, whereas it becomes relatively straight in larger specimens (IVPP V14530, IVPP V18637). Additionally, the caudal margin of the squamosal extends much further caudally than the parietals in small specimens (e.g., IVPP V18636 and IVPP V14530), but this difference is reduced in larger ones (IVPP V18637).

ACKNOWLEDGMENTS

The authors thank the members of the Sino-American expedition team for collecting the fossils described herein, and L.-S. Xiang, T. Yu, and X.-Q. Ding for preparing the fossils. Many thanks to editor A. Turner, and to P. Dodson and P. Makovicky, for their careful and insightful reviews of an earlier version of this paper. Collection of the fossils and subsequent research were funded by the National Natural Science Foundation of China (41120124002) to X. Xu, the National Geographic Society to J. Clark, the U.S. National Science Foundation (EAR 0310217 and EAR 0922187) to J. Clark, C. Forster, and X. Xu, and the Fundamental Research Funds for the Central Universities (CUGL140806) to F.-L. Han.

LITERATURE CITED

Barrett, P. M., and F.-L. Han. 2009. Cranial anatomy of *Jeholosaurus shangyuanensis* (Dinosauria: Ornithischia) from the Early Cretaceous of China. Zootaxa 2072:31–55.

Brown, B., and E. M. Schlaikjer. 1940. The structure and relationships of *Protoceratops*. Annals of the New York Academy of Sciences 40:133–266.

Butler, R. J., and Q. Zhao. 2009. The small-bodied ornithischian dinosaurs *Micropachycephalosaurus hongtuyanensis* and *Wannanosaurus yansiensis* from the Late Cretaceous of China. Cretaceous Research 30:63–77.

Butler, R. J., P. Upchurch, and D. B. Norman. 2008. The phylogeny of the ornithischian dinosaurs. Journal of Systematic Palaeontology 6:1–40.

Chinnery, B. J., and D. B. Weishampel. 1998. *Montanoceratops cerorhynchus* (Dinosauria: Ceratopsia) and relationships among basal neoceratopsians. Journal of Vertebrate Paleontology 18:569–585.

Chinnery-Allgeier, B. J., and J. I. Kirkland. 2010. An update on the paleobiogeography of ceratopsian dinosaurs; pp. 387–404 in M. J. Ryan, B. J. Chinnery-Allgeier, and D. A. Eberth (eds.), New Perspectives on Horned Dinosaurs: The Royal Tyrrell Museum Ceratopsian Symposium. Indiana University Press, Bloomington, Indiana.

Clark, J. M., X. Xu, D. A. Eberth, C. A. Forster, M. Machlus, S. Hemming, Y. Wang, and R. Hernández. 2006 The Middle-to-Late Jurassic terrestrial transition: new discoveries from the Shishugou Formation, Xinjiang, China; pp. 153 in P. M. Barrett and S. E. Evans (eds.), Ninth International Symposium Mesozoic Terrestrial Ecosystems and Biota, Manchester, UK, June 2006. Cambridge Publications, Natural History Museum, London.

Cooper, M. R. 1985. A revision of the ornithischian dinosaur *Kangnasaurus coetzeei* Haughton, with a classification of the Ornithischia. Annals of the South African Museum 95:281–317.

Dodson, P. 1990. Marginocephalia; pp. 562–563 in D. B. Weishampel, P. Dodson, and H. Osmólska (eds.), The Dinosauria. University of California Press, Berkeley, California.

Dodson, P., C. A. Forster, and S. D. Sampson. 2004. Ceratopsidae; pp. 494–513 in D. B. Weishampel, P. Dodson, and H. Osmólska (eds.), The Dinosauria, second edition. University of California Press, Berkeley, California.

Dodson, P., H.-L. You, and K. Tanoue. 2010. Comments on the basicranium and palate of basal ceratopsians; pp. 221–233 in M. J. Ryan, B. J. Chinnery-Allgeier, D. A. Eberth, and P. E. Ralrick (eds.), New Perspectives on Horned Dinosaurs: The Royal Tyrrell Museum Ceratopsian Symposium. Indiana University Press, Bloomington, Indiana.

Dong, Z.-M. 1989. On a small ornithopod (*Gongbusaurus wucaiwanensis* sp.nov.) from Kelamaili, Juggar Basin, Xinjiang, China. Vertebrata PalAsiatica 27:140–146. [Chinese with English summary].

Dong, Z.-M., and Y. Azuma. 1997. On a primitive neoceratopsian from the Early Cretaceous of China; pp. 68–89 in Z.-M. Dong (eds.), Sino-Japanese Silk Road Dinosaur Expedition. China Ocean Press, Beijing, China.

Evans, D. C., C. M. Brown, M. J. Ryan, and K. Tsogtbaatar. 2011. Cranial ornamentation and ontogenetic status of *Homalocephale calathocercos* (Ornithischia: Pachycephalosauria) from the Nemegt Formation, Mongolia. Journal of Vertebrate Paleontology 31:84–92.

Gradstein, F. M., J. G. Ogg, M. Schmitz, and G. Ogg. 2012. The Geologic Time Scale 2012, 2-volume set. Elsevier, Boston.

Han, F.-L. 2009. Anatomy of *Jeholosaurus shangyuanensis* and phylogenetic analysis of basal Ornithischia. M.S. thesis, Institute of Vertebrae Paleontology and Paleoanthropology Chinese Academy of Sciences, Beijing, China, 133 pp. [Chinese with English summary].

Han, F.-L., P. M. Barrett, R. J. Butler, and X. Xu. 2012. Postcranial anatomy of *Jeholosaurus shangyuanensis* (Dinosauria, Ornithischia) from the Lower Cretaceous Yixian Formation of China. Journal of Vertebrate Paleontology 32:1370–1395.

Jia, C. K., C. A. Forster, X. Xu, and J. M. Clark. 2007. The first stegosaur (Dinosauria, Ornithischia) from the Upper Jurassic Shishugou Formation of Xinjiang, China. Acta Geologica Sinica 81: 351–356.

Jin, L.-Y., J. Chen, S. Zan, R. J. Butler, and P. Godefroit. 2010. Cranial anatomy of the small ornithischian dinosaur *Changchunsaurus parvus* from the Quantou Formation (Cretaceous: Aptian-Cenomanian) of Jilin Province, northeastern China. Journal of Vertebrate Paleontology 30:196–214.

Kuiper, K. F., A. Deino, F. J. Hilgen, W. Krijgsman, P. R. Renne, and J. R. Wijbrans. 2008. Synchronizing rock clocks of earth history. Science 320:500–504.

Makovicky, P. J. 2001. *Montanoceratops cerorhynchus* (Dinosauria: Ceratopsia) braincase from the Horseshoe Canyon Formation of Alberta; pp. 243–262 in D. Tanke and K. Carpenter (eds.), Mesozoic Vertebrate Life. Indiana University Press, Bloomington, Indiana.

Makovicky, P. J., and M. A. Norell. 2006. *Yamaceratops dorngobiensis*, a new primitive ceratopsian (Dinosauria: Ornithischia) from the Cretaceous of Mongolia. American Museum Novitates 3530:1–42.

Marsh, O. 1890. Additional characters of the Ceratopsidae with notice of new Cretaceous dinosaurs. American Journal of Science (Series 3) 39:418–426.

Maryańska, T., and H. Osmólska. 1974. Pachycephalosauria, a new suborder of ornithischian dinosaurs. Palaeontologica Polonica 30:45–102.

Maryańska, T., and H. Osmólska. 1985. On ornithischian phylogeny. Acta Palaeontologica Polonica 30:137–150.

Maryańska, T., R. E. Chapman, and D. B. Weishampel. 2004. Pachycephalosauria; pp. 464–477 in D. B. Weishampel, P. Dodson, and H. Osmólska (eds.), The Dinosauria, second edition. University of California Press, Berkeley, California.